

1 **Main Manuscript for**

2

3 **Climate, demography, immunology, and virology combine to drive two decades of**
4 **dengue virus dynamics in Cambodia**

5

6 Cara E. Brook^{1*}, Carly Rozins², Jennifer A. Bohl³, Vida Ahyong⁴, Sophana Chea⁵, Liz
7 Fahsbender⁶, Rekol Huy⁷, Sreyngim Lay⁵, Rithea Leang⁷, Yimei Li¹, Chanthap Lon⁵, Somnang
8 Man^{5,7}, Mengheng Oum⁵, Graham R. Northrup⁸, Fabiano Oliveira³, Andrea R. Pacheco⁵, Daniel
9 M. Parker^{9,10}, Katherine Young¹¹, Michael Boots¹², Cristina M. Tato⁴, Joseph L. DeRisi⁴, Christina
10 Yek³, Jessica E. Manning^{3,5}

11

12 **Affiliations:**

13 ¹ Department of Ecology and Evolution, University of Chicago, Chicago, Illinois, USA

14 ² Department of Science and Technology Studies, York University, Toronto, Canada

15 ³ Laboratory of Malaria and Vector Research, National Institute of Allergy and Infectious
16 Diseases, National Institutes of Health, Rockville, Maryland, USA

17 ⁴ Chan Zuckerberg Biohub, San Francisco, California, USA

18 ⁵ International Center of Excellence in Research, National Institute of Allergy and Infectious
19 Diseases, National Institutes of Health, Phnom Penh, Cambodia

20 ⁶ Chan Zuckerberg Initiative, San Francisco, California, USA

21 ⁷ National Center for Parasitology, Entomology, and Malaria Control, Phnom Penh, Cambodia

22 ⁸ Center for Computational Biology, University of California, Berkeley, California, USA

23 ⁹ Department of Population Health and Disease Prevention, University of California, Irvine,
24 California, USA

25 ¹⁰ Department of Epidemiology and Biostatistics, University of California, Irvine, California, USA

26 ¹¹ Department of Biological Sciences, University of Texas, El Paso, Texas, USA

27 ¹² Department of Integrative Biology, University of California, Berkeley, California, USA

28

29 *Corresponding author: Cara E. Brook

30 Email: cbrook@uchicago.edu

31

32 **Author Contributions:** CEB and JEM conceived the study. JEM, JAB, HR, RL, and SC
33 conducted the febrile surveillance study and collected samples for mNGS in 2019-2022. VA,
34 CMT, JLD, JAB, SC, SL, CY, OM, SM, and JEM carried out RT-qPCR to identify dengue-positive
35 samples, as well as library preparation and mNGS. Other ancillary demographic data collection

36 and analyses were performed by RL, KS, CY, FO, and ARP. DP, CL, and JEM set up geospatial
37 system for patients. CEB and JAB generated consensus dengue genomes for upload to NCBI.
38 CEB carried out all TSIR, FOI, phylogenetic, and simulation analysis, with help from KY, YL, GN,
39 CR, and MB. CR and CEB extended the catalytic model to include waning multitypic immunity.
40 CEB and JEM wrote the first draft of the manuscript. All authors approved and contributed to
41 subsequent drafts of the manuscript and agree with the results presented.

42

43 **Competing Interest Statement:** No competing interests.

44 **Classification:** Biological Sciences / Population Biology

45 **Keywords:** dengue, genomic epidemiology, force of infection, wavelet decomposition

46

47 **This PDF file includes:**

48 Main Text

49 Figures 1 to 5

50

51

52

53

54

55

56

57

58

59

60

61

62

63

64

65

66

67

68

69

70

71

72 **ABSTRACT**

73

74 The incidence of dengue virus disease has increased globally across the past half-century, with
75 highest number of cases ever reported in 2019. We analyzed climatological, epidemiological, and
76 phylogenomic data to investigate drivers of two decades of dengue in Cambodia, an understudied
77 endemic setting. Using epidemiological models fit to a 19-year dataset, we first demonstrate that
78 climate-driven transmission alone is insufficient to explain three epidemics across the time series.
79 We then use wavelet decomposition to highlight enhanced annual and multiannual synchronicity
80 in dengue cycles between provinces in epidemic years, suggesting a role for climate in
81 homogenizing dynamics across space and time. Assuming reported cases correspond to
82 symptomatic secondary infections, we next use an age-structured catalytic model to estimate a
83 declining force of infection for dengue through time, which elevates the mean age of reported
84 cases in Cambodia. Reported cases in >70 year-old individuals in the most recent 2019 epidemic
85 are best explained when also allowing for waning multitypic immunity and repeat symptomatic
86 infections in older patients. We support this work with phylogenetic analysis of 192 dengue virus
87 (DENV) genomes that we sequenced between 2019-2022, which document emergence of DENV-
88 2 Cosmopolitan Genotype-II into Cambodia. This lineage demonstrates phylogenetic
89 homogeneity across wide geographic areas, consistent with invasion behavior and in contrast to
90 high phylogenetic diversity exhibited by endemic DENV-1. Finally, we simulate an age-structured,
91 mechanistic model of dengue dynamics to demonstrate how expansion of an antigenically distinct
92 lineage that evades preexisting multitypic immunity effectively reproduces the older-age infections
93 witnessed in our data.

94

95 **CLINICAL TRIAL NUMBERS:** NCT04034264 and NCT03534245.

96

97 **SIGNIFICANCE STATEMENT**

98 The year 2019 witnessed the highest number of dengue cases ever reported, including in
99 Cambodia, a Southeast Asian country with endemic transmission. We analyzed 19 years of
100 national dengue surveillance data for Cambodia to demonstrate how increasing temperature and
101 precipitation enhance similarity in dengue incidence across space and time, particularly in
102 epidemic years. We document how two decades of demographic transition has depressed the
103 rate at which dengue infections are acquired, thus increasing the age of reported infection. In
104 2019, expansion of a genetically distinct DENV-2 lineage into Cambodia likely underpinned
105 repeated symptomatic infections in older-age individuals to drive high caseloads. As climates
106 warm, we anticipate more synchronized dynamics globally and a shifting burden of symptomatic
107 disease into older cohorts.

108 **MAIN TEXT**

109

110 **INTRODUCTION**

111 Dengue virus (DENV) transmission has increased dramatically over the past two
112 decades, culminating in 2019 with the highest number of global cases ever reported (>5.2 million)
113 to the World Health Organization (WHO) (1). Since nearly three-quarters of DENV infections are
114 estimated to be clinically inapparent (thereby unreported), these counts represent a vast
115 underestimate of the true scale of dengue burden (2). DENV is a flavivirus primarily transmitted
116 by the *Aedes aegypti* mosquito, an ubiquitous arthropod vector in tropical and subtropical regions
117 (2). DENV is comprised of four antigenically distinct serotypes—each of which is further
118 subdivided among four to seven distinct genotypes; infection with one serotype is thought to
119 result in lifelong immunity to that same serotype (homotypic immunity) but only temporary (up to
120 two-year) protection against different serotypes (heterotypic immunity) (3). Heterotypic secondary
121 infections are often more clinically severe due to an interaction with pre-existing flavivirus-specific
122 antibodies known as antibody-dependent enhancement (ADE) (4, 5). Southeast Asia (SEA)
123 reports ~70% of dengue cases globally (1). Historically, dengue has been classified as an urban
124 disease, though recent studies highlighting the importance of microscale transmission in
125 generating DENV diversity in urban Bangkok predict that DENV transmission will intensify across
126 SEA as peri-urban settings become better connected (6–8). Cambodia, at a population size of 16
127 million, is currently the least urbanized country in SEA (9) but exhibits significant peri-urban
128 sprawl surrounding major metropolitan centers like the capital city, Phnom Penh (6, 7, 9).
129 Urbanization and climatic changes are increasing the population at-risk for dengue in Cambodia
130 and elsewhere (10–12).

131 Dengue was first detected in Cambodia in 1963 (13), though political instability and civil
132 war in the late 1970s delayed formalization of a passive surveillance policy until 1980 (14). Once
133 adopted, this policy required reporting of clinically diagnosed cases from public health centers
134 and hospitals to the national level. In 2001, the National Dengue Control Program (NDCP) was

135 inaugurated in Cambodia, and in 2002, the NDCP formally implemented the WHO clinical case
136 definitions of dengue and its complications as criteria for the surveillance program (14, 15). The
137 NDCP surveillance system is largely limited to clinicosyndromic diagnoses, meaning that
138 documented cases often correspond to more severe heterotypic secondary DENV infections (16),
139 which are reported collectively without the ability to systematically distinguish serotypes (15).
140 Nonetheless, the NDCP also instituted some active surveillance efforts in Cambodia in 2001,
141 which included limited molecular testing to identify distinct serotypes at sentinel sites in four
142 provinces, which were expanded to 15 provinces by 2021 (14, 15).

143 Over the past two decades, all four dengue serotypes have been detected in Cambodia
144 by molecular surveillance (15), though cases have been largely dominated by one or two
145 serotypes in a given year—with DENV-1 and DENV-3 most common in the early 2000s and
146 DENV-1 and DENV-2 predominant in the last decade (15). Cambodia witnessed three major
147 dengue epidemics across this period—in 2007, 2012, and 2019 (15). The first epidemic, in 2007,
148 occurred coincidentally with a genotype replacement event in DENV-1 (17, 18), though cases
149 were dominated by DENV-3, marking the last year of this serotype's dominance in the region (14,
150 18). The second epidemic, in 2012, has been largely attributed to DENV-1 (15, 19–21), and the
151 third, in 2019, appears to have been driven by co-circulation of both DENV-1 and DENV-2 (15).
152 Consistent with the global trends (1), Cambodia suffered its worst dengue epidemic on record in
153 2019, with approximately 40,000 total cases reported across all 25 provinces—a likely drastic
154 underestimation of the true disease burden (22). The past twenty years of surveillance in
155 Cambodia have witnessed, on average, steadily increasing dengue incidence, coupled with a
156 steady increase in the mean age of reported dengue infection (15). The increased age of reported
157 infection has been anecdotally attributed to an aging population following demographic transition,
158 as similar phenomena have been documented previously in neighboring Thailand (23, 24) and in
159 Nicaragua (25).

160 Explosive periodic outbreaks are a hallmark of dengue virus disease, though the multiple
161 drivers of these phenomena have long been debated (24, 26–29). Seasonal climate cycles are a

162 strong predictor of annual cycling for many arboviruses, including dengue (10, 11), and climate
163 has been implicated as a possible driver of multiannual dengue periodicity, as well. In Thailand,
164 multiannual dengue cycles demonstrate coherence with El Niño phenomena (29), and epidemic
165 years exhibit more synchronized dynamics across latitudes (29), as well as higher correlation with
166 local temperature than do inter-epidemic periods (28). The interaction of demography and
167 heterotypic immunity is also thought to play a role in driving multiannual dengue cycles (24, 26,
168 30), which, in Thailand, show elongated periodicity as a result of declining birth rates and slower
169 build-up of the susceptible population over the past half-century (24). Virology also contributes to
170 dengue epidemics, which have, historically, been linked to turnover in the dominant regional
171 serotype (31–33) or to replacement of a dominant viral genotype within a single serotype (18, 34).
172 Genotype-specific antigenic diversity is increasingly recognized within traditional serotype
173 classifications for dengue (35), and recent work links the magnitude of periodic dengue epidemics
174 to this antigenic evolution (34, 35). Large epidemics tend to result from the takeover of DENV
175 lineages most antigenically distinct from previously circulating strains of the same serotype or
176 most antigenically similar to lineages of a different serotype (34).

177 Here, we explore the dynamics of dengue virus transmission across the past two
178 decades in peri-urban Cambodia, investigating the potential mechanisms that underly periodic
179 epidemics, particularly the epidemic of 2019. We queried a 19-year dataset (2002-2020) of
180 serotype-agnostic dengue case counts from the NDCP, aggregated at the province level, to, first,
181 interrogate the role that climate played in driving epidemics in 2007, 2012, and 2019, and second,
182 more generally, explore the impact of climate on annual and multiannual cycling across the time
183 series. We, third, fit catalytic models to the age-structured incidence of reported dengue disease
184 to estimate the annual force of infection (FOI), at the province level, across this time series (24,
185 36, 37), then considered the national data in the context of our own active febrile surveillance
186 study carried out in peri-urban Kampong Speu and surrounding provinces from 2019-2022 (38).
187 Whole genome sequencing of DENV from serum samples collected in our active surveillance
188 program, combined with additional sequences from NDCP surveillance, identified the first record

189 of the DENV-2 Cosmopolitan lineage (Genotype-II (39)) ever documented in Cambodia (40).
190 Phylodynamic analysis of the spread of the DENV-2 Cosmopolitan lineage in this region suggests
191 that this genotype caused pathogenic infections in older age individuals, contributing to the
192 largest documented dengue outbreak on record for Cambodia in 2019. Finally, we constructed an
193 age-structured discrete-time, dynamical model to simulate the interplay of climate, demography,
194 immunology, and virology which combine to structure two decades of dengue dynamics in
195 Cambodia.

196

197 RESULTS

198 **Though warming temperatures correlate with increasing dengue incidence in Cambodia,**
199 **epidemic years are not consistent climate anomalies.**

200 Because of the widely acknowledged role of climate as a driver of arboviral disease
201 globally (10, 11), coupled with recent work from Thailand that highlights coherence between El
202 Niño climate anomalies and dengue epidemics (29), we first explored the influence of changing
203 temperature and precipitation on dengue caseload in Cambodia. To this end, we aggregated
204 high-resolution temperature and precipitation data at the Cambodian province level, across two-
205 week intervals from 2002-2019 and sought to address the extent to which epidemic years
206 represented climatic anomalies over this time period; we defined 'anomalies' as any years in
207 which temperature or precipitation records demonstrated significant deviations from average
208 trends through time, as calculated using generalized additive models (GAMs) (41). Across the
209 time series, temperature peaked in the first half of each year, between April and July, preceding
210 the peak in dengue caseload (Fig. S1). Precipitation peaked in the latter half of each year,
211 between August and October (Fig. S2), preceding the onset of the following year's dengue
212 season. GAMs (41) demonstrated that, after controlling for intra-annual variation, temperature
213 has increased significantly across the past two decades in all provinces; no significant interannual
214 changes were detected for precipitation (Fig. S3-S4; Table S1). Additional GAMs and climate
215 data normalized into z-scores indicated that the epidemic years of 2012 and 2019 were

216 anomalously warm, while 2007 was anomalously cool, consistent with the observed interannual
217 increase in temperature (Fig. S5). Years 2015-2016, which spanned a major El Nino event in
218 SEA (but did not correspond to a dengue epidemic in Cambodia) (42), were also significantly
219 warmer than average. By contrast, precipitation showed no anomalies in the year preceding each
220 of the three major dengue epidemics (Fig. S6). We concluded that, while both temperature and
221 dengue incidence increased across our time series, epidemic years could not be consistently
222 distinguished by any consistently aberrant climatic profile.

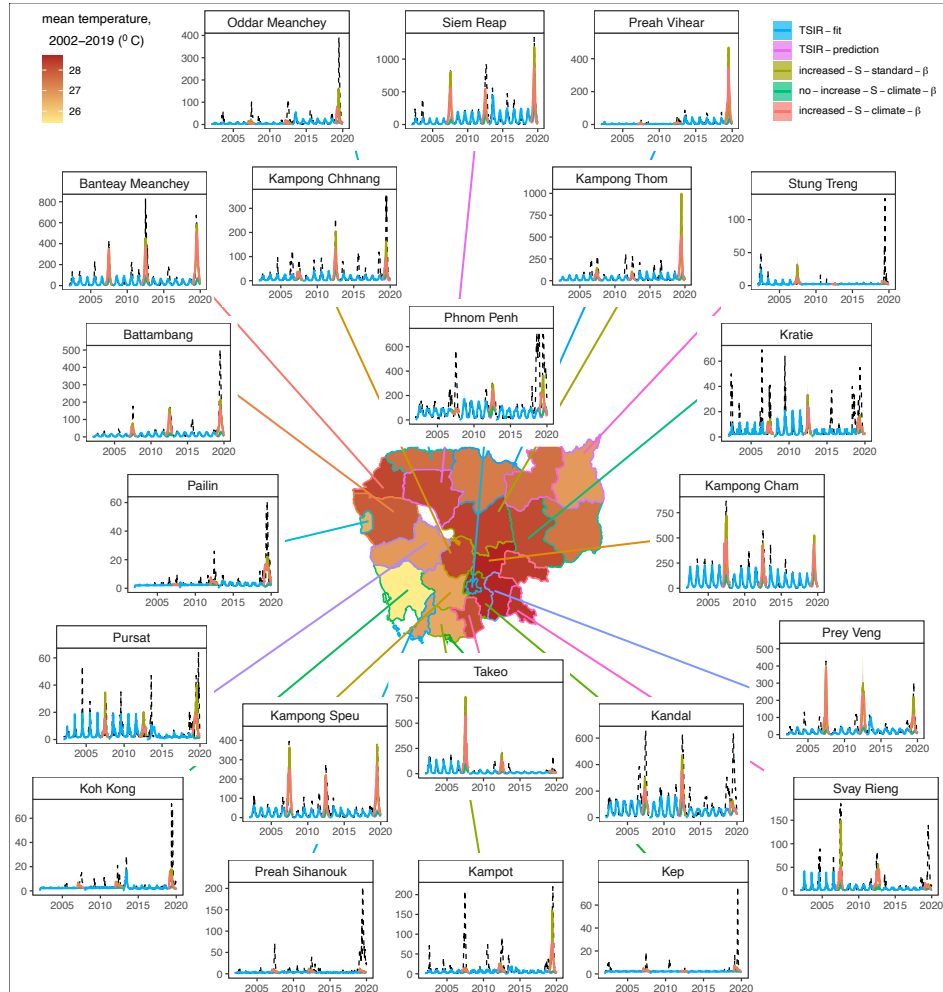
223

224 **Climate-informed transmission rates failed to recover epidemic dynamics in a TSIR model.**

225 To formally interrogate the role of climate as a driver of dengue epidemics in Cambodia,
226 we developed a simple, climate-informed time series Susceptible-Infected-Recovered (TSIR)
227 model (43–45), which we fit to dengue case counts, aggregated over two week intervals at the
228 province level, for the three inter-epidemic periods (2002-2006, 2008-2011, and 2013-2018).
229 Typically used to describe the transmission dynamics of perfectly immunizing childhood
230 infections, such as measles (44, 45), TSIR has been applied to dengue dynamics previously and
231 offers an effective means by which to isolate the impact of climate on transmission, despite
232 oversimplifying the multiple serotype dynamics of dengue virus disease (46–50).

233 We used biweekly transmission rates recovered from TSIR fits to the inter-epidemic
234 periods, as well as climate-informed transmission rates for epidemic years projected from
235 province-specific lagged temperature and precipitation data, to predict epidemic-year cases (Fig.
236 1; *Methods; SI Appendix*). We found that TSIR successfully recaptured the timing of annual
237 dengue epidemics across the 22 provinces considered, with the recovered transmission rate
238 peaking between May and August, slightly preceding reported cases. The magnitude and timing
239 of transmission varied by province and between the three inter-epidemic periods, showing no
240 consistent pattern of directional change in magnitude with time (Table S2). TSIR-estimated
241 transmission was significantly positively associated with higher temperature and precipitation
242 (lagged such that climate variables preceded transmission by a median 3.5 months for

temperature and 1 month for precipitation) in the corresponding province across all inter-epidemic periods (Table S3-S4). More rapid transmission gains were observed for corresponding increases in temperature vs. precipitation (Fig. S7-S9; Table S4). Nonetheless, climate-informed transmission rates for epidemic years were not substantially different from rates fitted to inter-epidemic periods, reflecting the absence of major climate anomalies across the time series (Fig. S10).



249

250 **Figure 1. Climate-informed TSIR insights into epidemic dynamics of DENV in Cambodia.** Inset panels
 251 show province level clinicosyndromic reported DENV cases (*dashed black lines*) with fitted TSIR output to
 252 the three inter-epidemic periods (2002-2006, 2008-2011, 2013-2018; *blue lines*) and TSIR projections for
 253 epidemic years (2007, 2012, 2019) under trained biweekly transmission rate (β) estimates (*pink lines*),
 254 incorporating a factorial increase in the susceptible population (*gold lines*), using a climate-projected β
 255 estimated from lagged temperature and precipitation data by province (*green lines*), or using both climate-
 256 projected β and a factorial increase in the susceptible population (*red lines*) (SI Appendix, Table S2, S5).
 257 The center map shows province level administrative boundaries for Cambodia, shaded by the mean
 258 biweekly temperature in 2020.

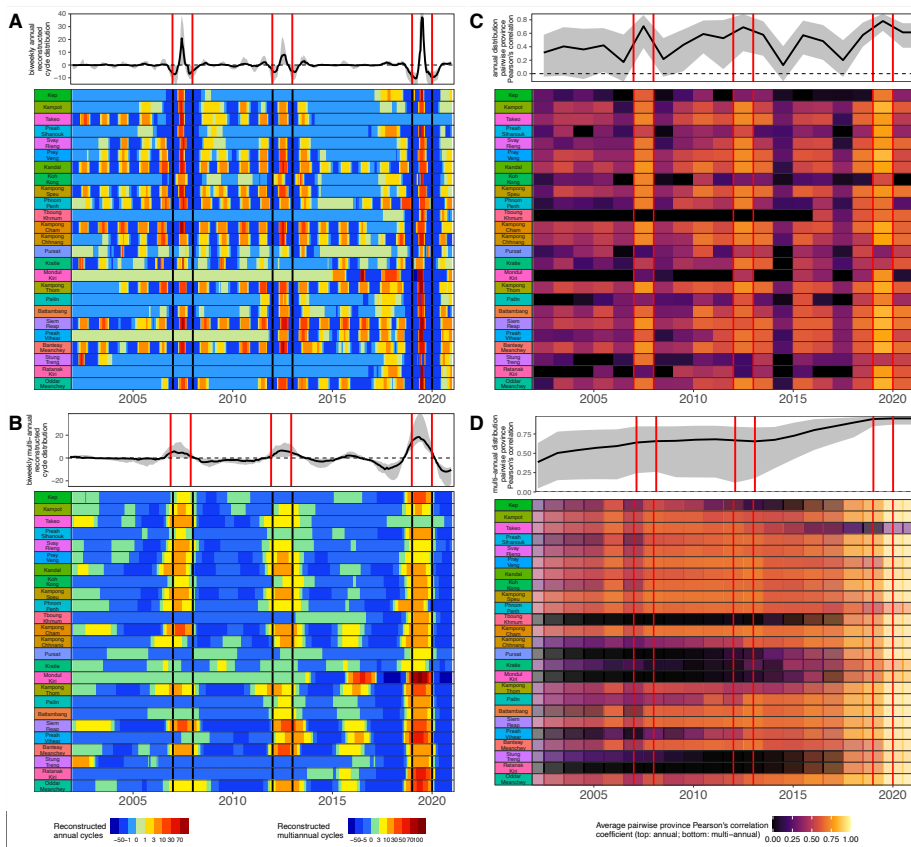
259 As expected, TSIR underpredicted the magnitude of epidemic year caseloads for all
260 provinces; climate-informed transmission improved TSIR projections but still failed to recover
261 epidemic peaks (Fig. 1). Experimentally, we amplified the susceptible population input at the
262 beginning of each epidemic year in our model, which facilitated recovery of DENV caseloads
263 (*Methods*) (50). In the absence of climate input into the transmission rate, the proportional
264 increase in susceptible population at the beginning of each epidemic year needed to recover the
265 epidemic peak was a median 1.8x for 2007, 2.10x for 2012, and 2.17x for 2019 (Table S5). The
266 proportional increase in the susceptible population needed to recover the epidemic peak was not
267 significantly lower when epidemic year cases were projected using climate-informed transmission
268 rates for 2007 and 2012 (paired student's t-test: [2007] $t=0.33$, $p>0.1$; [2012] $t=-0.52$; $p>0.1$) and
269 only marginally lower for 2019 ($t=1.31$, $p=0.1$), suggesting (at most) a minimal role for
270 temperature and precipitation in driving epidemic dynamics (Table S5). For many provinces, the
271 combination of climate-informed transmission rate with susceptible augmentation still fell short of
272 effectively capturing epidemic caseloads, highlighting the need for alternative explanations for
273 these high transmission years.

274

275 **Wavelet analysis showed enhanced synchrony in dengue dynamics across provinces and**
276 **climate time series in epidemic years.**

277 Though TSIR modeling failed to recover a clear role for climate in driving major dengue
278 epidemics in Cambodia, the analysis did highlight a critical influence of climate on the intraannual
279 timing of cases and the interannual periodicity of dengue dynamics. Prior work in Thailand has
280 demonstrated enhanced synchronicity between dengue incidence and climate, and between
281 geographically distant localities, during major epidemics (28, 29), as well as a link between
282 multiannual climate cycles and higher burden epidemics (29). We hypothesized that these
283 multiannual climate cycles not considered in TSIR might also be important in the Cambodia
284 system. To this end, we undertook wavelet decomposition of the biweekly dengue time series and
285 the corresponding climate data, both at the province level, to extract and disaggregate annual

286 and multiannual trends. We found elevated amplitude and statistically significant peaks in
287 average wavelet power of both annual (Fig. 2A, S11A) and multiannual (Fig. 2B, S11B) cycles in
288 dengue incidence during the three epidemic years (51). Elevated amplitudes for multiannual
289 cycles were also observed during the 2015-2016 El Niño event in more northerly provinces (Fig.
290 2B), including those abutting Thailand, where associations between dengue and El Niño have
291 been previously established (29). We additionally observed significantly elevated synchronicity
292 between provinces in the timing and amplitude of yearly dengue incidence across epidemic
293 years, as measured both by pairwise Pearson's correlation coefficient (Fig. 2C) and cross-
294 wavelet power (Fig. S11). Synchronicity in the annual incidence data was negatively associated
295 with geographic distance between provinces, though patterns were less clear than have been
296 described elsewhere (29) (Fig. S12). High synchronicity between annual case data for paired
297 provinces was significantly positively associated with high temperature, precipitation, and
298 population size of a focal province (Fig. S12; Table S6).



299
300 **Figure 2. Wavelet reconstructions show heightened synchrony in epidemic years. Reconstructed A**

301 annual and **B** multiannual dengue cycles by province, by year from NDCP incidence per 100,000 population.
302 **C** Mean pairwise Pearson's correlation coefficient (ρ) for annual dengue incidence between focal province
303 and all other provinces through time. **D** Mean ρ comparing province-to-province reconstructed multiannual
304 dengue cycles across a 5-year sliding window, with overlapping window frames plotted (partially translucent)
305 atop one another. In all panels, epidemic years are highlighted by vertical red or black bars. Top panels
306 indicate the distribution of corresponding values (median = solid line; max-to-min range = gray shading)
307 observed across all provinces within each timestep. X-axis labels are marked on January 1 of the
308 corresponding year.
309

310 For multiannual cycles, we observed a trend of steadily increasing synchronicity (Fig. 2D)
311 and cross-wavelet power (Fig. S11D) between provinces through time, though no peaks occurred
312 in epidemic years. Cross-wavelet power between raw dengue incidence and the corresponding,
313 province-level mean temperature and total precipitation (grouped biweekly) also peaked in
314 epidemic years (Fig. S13 AB). At the multiannual scale, cross-wavelet power between province-
315 level reconstructed dengue cycles and temperature and precipitation largely increased across the
316 time series (Fig. S13CD), though values were highest slightly preceding the 2019 epidemic and
317 overlapping the 2015-2016 El Niño event (42). The same pattern was observed when comparing
318 monthly reconstructed multiannual dengue cycles and the Oceanic Niño Incidence (ONI) (Fig.
319 S13E). For temperature, precipitation, and ONI, cross-wavelet power with multiannual dengue
320 cycles peaked earlier in the time series in more southern provinces and moved gradually
321 northward (Fig. S13C-E). All told, wavelet analyses suggested a role for climate in synchronizing
322 annual dengue epidemics across provinces, but only minimal support for a hypothesis of
323 multiannual climate cycles driving periodic epidemics across our time series. In contrast to reports
324 from two decades prior in Thailand (24), the periodicity of multiannual dengue cycles across
325 provinces did not increase in duration throughout our time series, despite decreasing birth rates
326 (Fig. S14). This perhaps reflects the relative slowdown in both birth and death rate declines in
327 Cambodia over the past two decades, when compared with the dramatic declines witnessed
328 twenty years prior (Fig. S14).

329

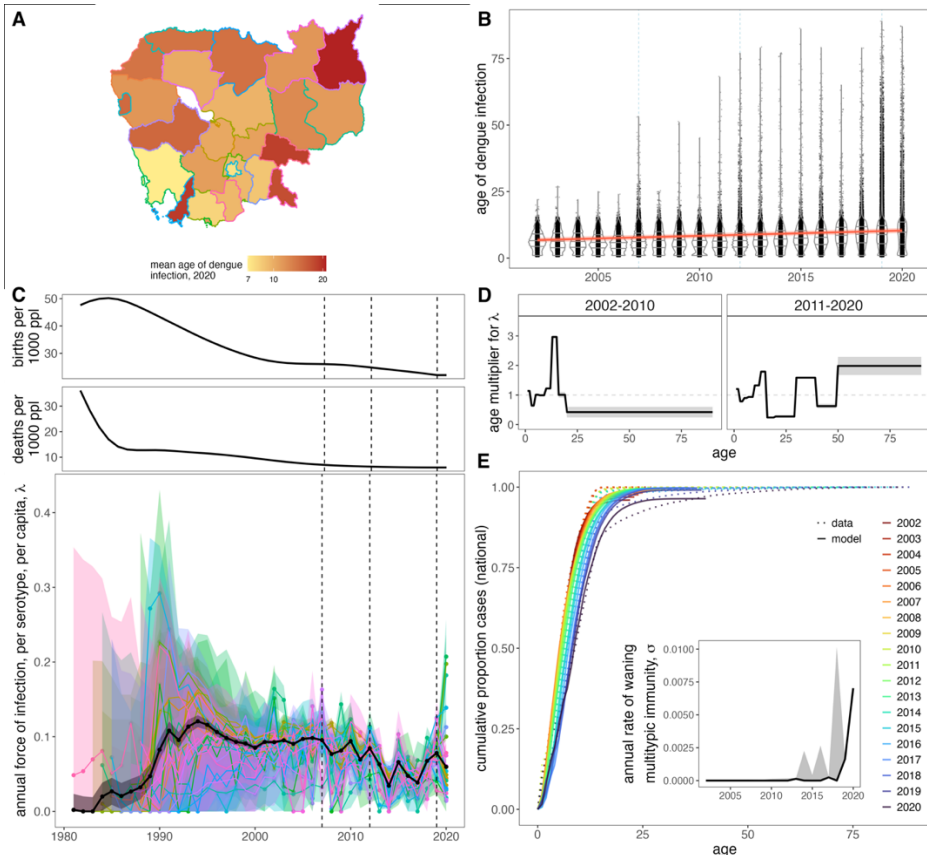
330

331

332 **Mean age of reported dengue infection increased across the study period, corresponding
333 to a declining force of infection.**

334 The muted effects of climate on our epidemic time series led us to next investigate
335 demographic and immunological drivers of dengue dynamics in Cambodia. Previous work has
336 documented a trend of increasing mean age of reported dengue infection across the past two
337 decades in Cambodia at the national level (15); we confirmed this to be consistent at the province
338 level (Fig. 3A,B; Fig. S15; Table S7). Nationally, the mean age of reported dengue infection
339 increased from 6.79 years (95% CI: 5.85-7.72) in 2002 to 10.34 years (95% CI: 9.41-11.27) in
340 2020 ($p < 0.001$). Increases in age of reported cases were even more dramatic in more remote
341 provinces: in the distant northeastern province of Mondul Kiri, for example, the mean reported
342 age of infection increased from 3.72 years (95% CI: 1.97-5.47) in 2002 to 21.18 years (95% CI:
343 20.84-21.53) in 2020 (Fig. 3A; Fig. S15; Table S7).

344



345
346 **Figure 3. Demographic transition underpins declining force of infection and increasing age of**

347 **reported dengue incidence in Cambodia. A** Mean age of reported dengue infection, by province in the
348 last year of the NDCP time series (2020). **B** Age distribution of reported dengue cases by year, with violin
349 plots highlighting changes in the interquartile range of cases. The interannual trend in the mean age of
350 dengue infection is plotted as a solid red line, with 95% confidence intervals by standard error shown as a
351 narrow, translucent band behind it (Table S7). Epidemic years (2007, 2012, 2019) are highlighted by a light
352 blue, dashed line in the background. **C** National (black) and province level (colored) estimates for the
353 annual, per serotype, per capita force of infection from 1981 to 2020. 95% confidence intervals from the
354 hessian matrix are shown as translucent shading. FOI estimates are compared against national birth and
355 death rates for Cambodia across the time series, with epidemic years highlighted by vertical dashed lines. **D**
356 Age modifiers to the FOI fit as shared across all provinces for 2002-2010 and 2011-2020 subsets of the
357 data, with 95% confidence intervals from the hessian matrix are shown as translucent shading. **E**
358 Cumulative increase in the proportion of cases reported by age at the national level, colored by year. Data
359 are shown as dotted lines and model output as solid lines. Model includes national FOI estimates from **C**,
360 age modification terms from **D**, and time-varying waning multitypic immunity as shown in the inset.
361

362 To interrogate the mechanistic drivers of this pattern, we estimated the annual force of
363 infection (FOI, or λ), the rate at which susceptibles become infected, by fitting a catalytic model
364 with multiple serotype exposures to the province level data for every year in the dataset (2002-
365 2020) and the 22 years preceding the onset of the time series, dating back to the birth year of the
366 oldest individual in the first year of the data (Fig. 3C) (24, 36, 37). As in previous models for
367 dengue (24, 36), we assumed that reported cases represented secondary, symptomatic
368 infections most likely to report to public hospitals and clinics. Resulting patterns in FOI by
369 province largely mirrored those recovered nationally (Fig. S16), demonstrating a consistently high
370 FOI in the early 1990s, corresponding to the years in which individuals born in Cambodia's 1980s
371 birth pulse (which followed severe population reductions from civil war in the 1970s) would likely
372 experience secondary infections. The FOI subsequently demonstrated a gradual decline across
373 the time series, interspersed with local peaks in epidemic years and in 2010 and 2015.
374

375 **Age-structured FOI modifications and waning multitypic immunity in 2019-2020 improved
376 the catalytic model's ability to recapture observed data.**

377 We next fit 19 multiplicative age modification parameters, shared across all provinces, to
378 allow for modulation of annual FOI across different age categories; eight age class were
379 considered for the first half of the time series and eleven for the second, corresponding to the
380 expanded age range of reported cases (Fig. 3D). Incorporation of age modifiers improved model
381 fits to the data across all provinces (Table S8). Consistent with recent work in Thailand (23), we

382 identified a high hazard of infection in adolescents (13-15 year-olds) across the time series. In the
383 second decade, we additionally noted an elevated age-specific hazard of infection in 30-39 year-
384 olds and >50 year-olds, corresponding to case reports in older cohorts.

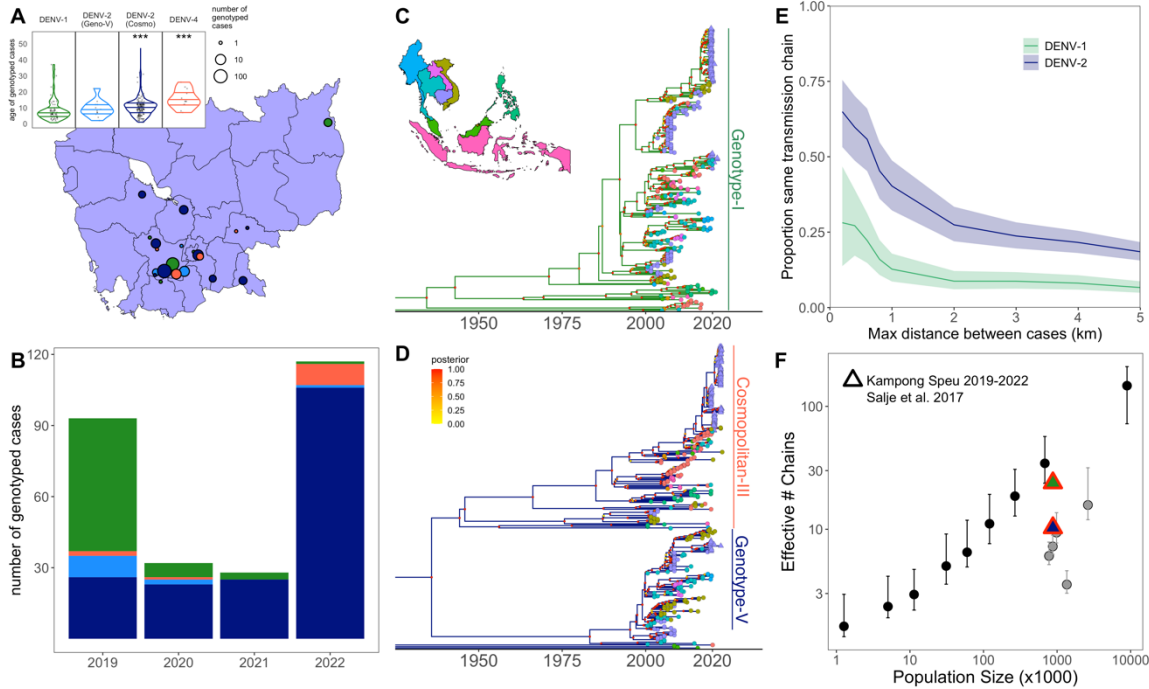
385 Because the age range of these older cases greatly exceeded average age increases
386 predicted by declining FOI, we reconsidered our original assumption by which reported cases
387 corresponded to clinically apparent secondary infections only. Visualization of the age distribution
388 of reported cases by year at both the national (Fig. 3B) and province levels (Fig. S15) indicated
389 that, in addition to increases in the mean reported age of dengue infection, the past two decades
390 of dengue incidence in Cambodia have also witnessed expansion in the age *range* of reported
391 cases—such that approximately 1% of reported cases (712/68597) in 2019 occurred in
392 individuals over the age of 45, with 61 infections reported in individuals >70 years in age. We also
393 observed an isolated spike in the age distribution of reported cases in some provinces in the
394 epidemic years of 2007 and 2012 (Fig. S15). To recapture these symptomatic infections in older
395 age-individuals, we modified the multitypic catalytic modeling framework presented in previous
396 work (24, 25, 36) to permit individuals to wane from a state of multitypic immunity back to that of
397 monotypic immunity subject to renewed hazard of symptomatic re-infection (*SI Appendix*). Using
398 this new modeling framework, we estimated a shared parameter across all provinces, which
399 corresponded to the rate of waning multitypic immunity (σ). When we allowed σ to vary by year,
400 we estimated a significant signature of waning multitypic immunity in the 2019 and 2020 data only
401 (Fig. 3E, *inset*). Incorporating time-varying σ improved model fit when added both to the FOI-only
402 model and the FOI model modified by age class (Table S8). Our best fit FOI model including both
403 age modifications and time-varying multitypic waning immunity effectively recaptured the
404 observed cumulative proportion of cases per age class per year at national (Fig. 3E) and province
405 (Fig. S17) levels. In general, cases accumulated more slowly across age classes with advancing
406 years, tracking declining FOI.

407

408 **DENV genotyping from 2019-2022 suggests a likely DENV-2 clade replacement event in**
409 **Cambodia.**

410 The results of our FOI analysis led us to question whether regional turnover in the
411 dominant DENV virus lineage could underpin the 2019 signature of immunological naivety
412 identified in our data. Prior work emphasizes the key role that antigenic novelty, influenced by
413 both serotype and genotype, plays in determining fitness advantages for co-circulating DENV
414 variants (34, 35). To address this question in our system, we leveraged serum samples amassed
415 during an active febrile surveillance study that we carried out in Kampong Speu province,
416 adjacent to the Cambodian capital city of Phnom Penh, between July 2018 and December 2022
417 (38, 40). In this study, serum collected from patients reporting to the provincial referral hospital
418 within 24 hours of fever was subject to RNA extraction and metagenomic Next Generation
419 Sequencing (mNGS) to identify the etiology of infection (38, 40). We successfully identified
420 serotype and corresponding genotype from mNGS data for 239 DENV-positive Kampong Speu
421 cases. We supplemented these with samples collected from 11 cases identified in our more
422 limited active surveillance in five neighboring provinces in 2021-2022 and 20 cases identified in
423 routine NDCP surveillance across six provinces, also in 2021-2022 (Fig. 4A; Table S9). From this
424 data subset of positive DENV samples, we sequenced and submitted 192 whole DENV genomes
425 to NCBI (63 DENV-1, 120 DENV-2, and 9 DENV-4; Table S9), representing one-third of full
426 genome DENV-1 sequences and two-thirds of full genome DENV-2 sequences currently available
427 for Cambodia.

428
429
430



431
432 **Figure 4. Bayesian time trees highlight geospatial structuring in evolutionary relationships for**
433 **Cambodian dengue. A** Map of Cambodia with locations of DENV serum samples genotyped from 2019-
434 2022 in part with this study. Cases are grouped together within 10km radii. The centroid of each case cluster
435 is plotted, with circle size corresponding to sample number and shading corresponding to serotype and
436 genotype (DENV-1=green; DENV-2 Genotype-V = light blue; DENV-2 Cosmopolitan (Genotype-II) = navy;
437 DENV-4=orange). The age distribution of cases by serotype and genotype is shown in the upper left; DENV-
438 2 Cosmopolitan and DENV-4 infections occurred in significantly older age individuals than reference DENV-
439 1 infections (linear regression; $p<0.001$; Table S10). **B**. Number of genotyped DENV cases by year from
440 febrile surveillance in this study, colored by serotype and genotype as showing in panel A. **C** Map of
441 Southeast Asia with countries colored corresponding to sequences, as shown in tip points on phylogenetic
442 timetrees constructed using BEAST 2 for DENV-1 and **D** DENV-2. X-axis highlights divergence times
443 between corresponding sequences. Reference sequences from GenBank are represented as circle tips and
444 sequences contributed by active febrile surveillance in this study as triangles. Cambodia and corresponding
445 sequences are shaded purple. Clade bars indicate the genotype of corresponding sequences within each
446 serotype: genotype-1 for DENV-1 and Genotype-V and Cosmopolitan III (Genotype-II) for DENV-2. See Fig.
447 S19 for a detailed inset of geographic localities for 2019-2022 Cambodia sequences. **E** Proportion of
448 geolocated sequence pairs from panel A for DENV-1 (green) and DENV-2 (blue) genomes derived from the
449 same transmission chain across progressively longer Euclidean distances. **F** Number of effective
450 transmission chains for circulating DENV estimated across populations of varying densities. Black (urban)
451 and gray (rural) circles with corresponding 95% confidence intervals depict estimates for Thailand from Salje
452 et al. 2017 (8), while triangles depict estimates from our Kampong Speu active febrile surveillance study for
453 DENV-1 (green) and DENV-2 (blue).
454

455 Maximum likelihood phylogenetic analysis of the resulting genomes demonstrated that
456 most DENV-2 sequences recovered from our 2019-2022 study belonged to the DENV-2
457 Cosmopolitan III lineage (Genotype-II), the first record of this genotype in Cambodia, though its
458 emergence has been reported recently in several neighboring SEA countries (Fig. S18) (52-55).
459 All DENV-1 sequences clustered in the Genotype-1 lineage, consistent with previous genotype

460 records in Cambodia (Fig. S18). Genotyped cases from 2019 were largely split between DENV-1
461 (N=56/93, 60.2%) and DENV-2 (N=35/93, 37.6%) serotypes, while those from 2020-2022 were
462 dominated by DENV-2 (2020: N=25/32, 78.1%; 2021: 25/28, 89.3%; 2022: 107/117, 91.4%) (Fig.
463 4B). A small number of DENV-4 cases were also sequenced across the time series (Fig. 4B). The
464 Cosmopolitan III lineage (Genotype-II) of DENV-2 became increasingly prevalent across the time
465 series, as compared with the Genotype-V lineage previously recorded in Cambodia (Fig. 4B). The
466 Cosmopolitan lineage increased in prevalence from 74.3% (26/35) of DENV-2 cases in our study
467 in 2019 to 99.1% (106/107) of cases in 2022 (Fig. 4B). We additionally observed that the mean
468 age of infection was significantly higher for DENV-2 Cosmopolitan cases genotyped in our study
469 (while the mean age of DENV-2 Genotype-V infection showed no difference), as compared with
470 reference DENV-1 case (Fig. 4A; Table S10, p<0.001). Mean age of infection was also
471 significantly elevated for DENV-4, likely because it circulated at much lower prevalence.

472 We constructed serotype-specific Bayesian timetrees (56, 57) from full genome DENV
473 sequences to assess the divergence time of 2019-2022 lineages from sequences previously
474 reported from Cambodia and neighboring SEA countries between 2002-2022 (Fig. 4C-D; Table
475 S9). The majority of DENV-1 lineages recovered from our study in 2019-2022 clustered closely
476 with other DENV-1 sequences reported to NCBI from Cambodia across the past decade (Fig.
477 4C). By contrast, DENV-2 sequences in the Cosmopolitan III lineage (Genotype-II) demonstrated
478 high divergence from the most recently reported Genotype-V sequences for Cambodia, with a
479 time to most recent common ancestor (tMRCA) of approximately 77.1 years (Fig. 4D; MRC: 1945,
480 95% HPD: 1942-1949). Locally, within our regional data subset, sequences collected from cases
481 coincident in geographic space and time were highly phylogenetically related (Fig. S19),
482 supporting previous studies emphasizing the importance of microscale transmission for DENV
483 (8). Nonetheless, we observed reduced phylogenetic diversity overall and a higher degree of
484 phylogenetic relatedness across wider geographic distances for DENV-2 vs. DENV-1 sequences,
485 consistent with a hypothesis of recent genotype invasion (Fig. 4E). Indeed, some 60% of paired
486 DENV-2 sequences separated by up to 400m of geographic distance were estimated to share a

487 MRCA within six months of the onset of the earlier case (corresponding to a shared 'transmission
488 chain'), as compared with only 22% of DENV-1 sequences. At a distance of up to 1 km
489 separation, some 40% of DENV-2 pairs still belonged to the same transmission chain, in contrast
490 to only 13% of DENV-1 sequences. Specifically for the Kampong Speu data, we additionally
491 estimated the number of distinct DENV-2 vs. DENV-1 effective transmission chains in circulation
492 in the region (Fig. 4F). When compared with prior work from neighboring Thailand, the number of
493 effective transmission chains per population size for DENV-1 in Kampong Speu closely matched
494 that predicted by population size in the endemic transmission setting of urban Bangkok (8). By
495 contrast, the lower number of transmission chains per population size estimated for DENV-2 was
496 closer to that previously observed in rural regions in Thailand with less continuous endemic
497 transmission (Fig. 4F).

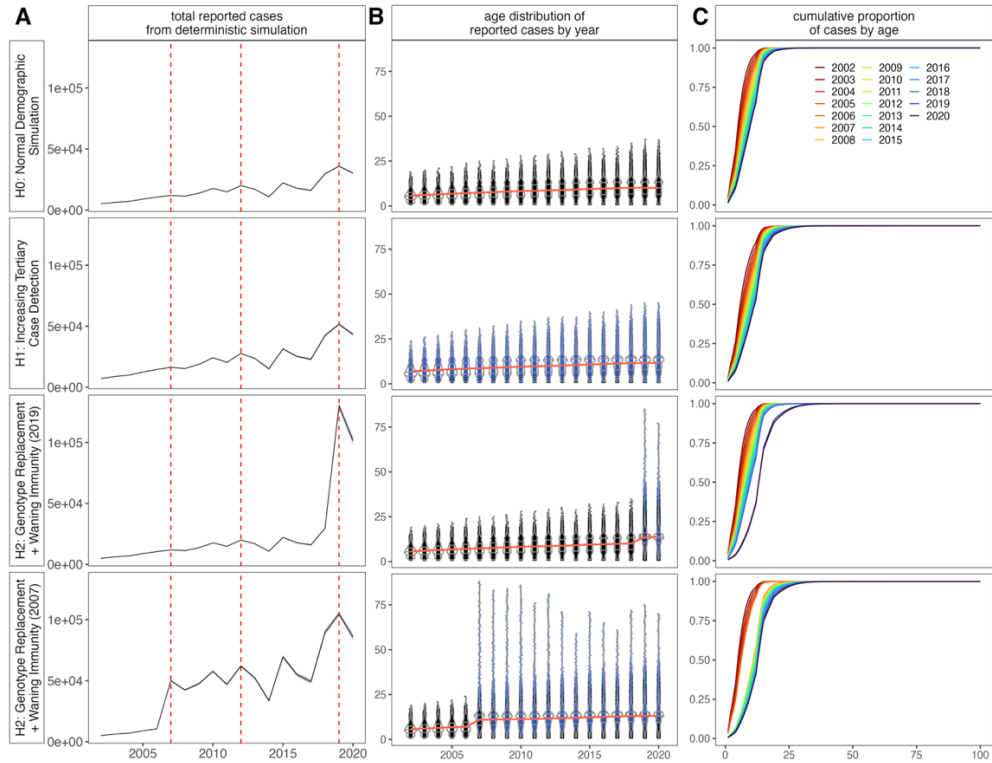
498 All told, our phylogenetic analyses describe the emergence of a previously unrecorded
499 genotype of highly divergent DENV-2 in at least ten different Cambodian provinces. This
500 genotype greatly increased in prevalence following its first record in Cambodia in 2019 and
501 caused infections in older-age individuals. The limited phylogenetic diversity observed from
502 DENV-2 sequences suggest that the Cosmopolitan lineage (Genotype-II) arrived relatively
503 recently to the region. Its high genetic divergence from previously reported genotypes in
504 Cambodia may be associated with antigenic novelty that played a role in the 2019 epidemic.

505
506 **Mechanistic simulations of clade replacement with antigenic escape in an age-structured
507 model recapture patterns witnessed in the data.**

508 Combined, our FOI analysis and genotyping suggest that the DENV-2 Cosmopolitan
509 lineage (Genotype-II) caused a genotype replacement event in Cambodia, which likely played a
510 part in the 2019 epidemic in the region. The higher burden of cases in older age individuals more
511 likely to have some form of pre-existing dengue immunity additionally suggested that the
512 Cosmopolitan genotype may be sufficiently antigenically divergent to overcome this immunity,
513 resulting in symptomatic infection. To formally evaluate this hypothesis, we constructed a

514 mechanistic, age-structured discrete time deterministic epidemic model in biweekly timesteps (S/
515 *Appendix*) (58–60), with which we simulated diverse mechanisms hypothesized to underpin
516 observed patterns in our data. We sought to explain both the general pattern of increasing
517 average age of reported infection through time, as well as the high caseload and wide distribution
518 in age range of cases associated with the 2019 epidemic (and, to a lesser extent, prior epidemic
519 years). Previous work in Thailand shows similar patterns of drastically older age infections in
520 more recent years, which the authors explain via a mechanism of increased detectability of
521 tertiary or quaternary infections through time (23). In practice, this mechanism is similar to our
522 extension of Ferguson et al. (1999)'s catalytic model for dengue, which incorporates waning
523 multitypic immunity, as both approaches allow for case detection in individuals experiencing more
524 than two dengue infections across their lifetime. We used our simulation model to evaluate
525 whether these two mechanisms were functionally distinguishable and, if so, which best replicated
526 Cambodian data.

527 For simplicity, we restricted ourselves to a three-serotype system and initiated
528 simulations incorporating seasonal variation in transmission as estimated by TSIR (Fig. 1) and
529 annual variation in FOI corresponding to national estimates (Fig. 3). As with our FOI analysis, we
530 modeled secondary infections as reported cases for (H0) normal demographic simulations. We
531 then compared these results against simulations of (H1) hypotheses that allowed for continuously
532 increasing detectability of tertiary cases through time or (H2) hypotheses of genotype
533 replacement paired with waning multitypic immunity and detectable reinfection within a serotype
534 (Fig. 5). We also compared (H3) hypotheses of genotype invasion with no lineage-specific waning
535 immunology or (H4) hypotheses of genotype invasion with continuous increasing tertiary case
536 detection, again not specific to the invading lineage (Fig. S21). We focused our analyses on
537 drivers of the 2019 epidemic but also conducted a subset of simulations to highlight insights
538 gleaned from the 2007 epidemic in Cambodia (Fig. 5, *bottom*).
539
540



541
542 **Figure 5. Simulations of genotype clade replacement recapitulate observed expansion in the age**
543 **structure of reported dengue cases from Cambodian data. A** Total reported cases (solid line = mean
544 FOI; translucent shading = 95% confidence interval for FOI), **B** age distribution of reported cases by year
545 (black = secondary; blue = repeat secondary or tertiary), and **C** cumulative proportion of reported cases by
546 age, from deterministic model simulations indicated to the left of panel A.
547

548 All simulations successfully recovered the pattern of increasing mean age of reported
549 infection, as witnessed in the data. This increase was steeper under (H1) assumptions of
550 increasing detectability for tertiary infections (Fig. 5). Because we parameterized FOI from the
551 national time series for Cambodia, for which the 2019 FOI was locally elevated (Fig. 3), all
552 simulations also effectively reproduced a higher burden of cases in 2019. Critically, we found that
553 sudden, sharp expansions in the age distribution of reported cases, as witnessed broadly across
554 provinces in epidemic years for Cambodia (Fig. S15), were only possible when modeling some
555 form of antigenic novelty for the invading lineage (H2; Fig. 5). Simulations of this novel antigenic
556 invasion in 2007 (Fig. 5 H2, bottom) also demonstrated how the expanded age distribution should
557 subsequently narrow in the years following clade replacement with immune evasion, again
558 consistent with Cambodian data (Fig. S15). By contrast, (H1) hypotheses of constant increasing
559 tertiary case detection through time will only continue to expand this distribution over longer time

560 horizons. Importantly, modeling of genotype turnover had no demonstrable impact on the age
561 distribution of cases in the absence of *specific* enhanced detectability for the invading clade, even
562 when allowing for generally heightened tertiary case detection through time (Fig. S21). Thus, we
563 conclude that only introduction of antigenically divergent genotypes (or, of course, serotypes) can
564 be expected to generate this dramatic short-term expansion in the age distribution of cases.
565 Notably, our results were agnostic to classification of repeat infections with an invading lineage as
566 tertiary detections (e.g. detection of DENV-2 infection following prior exposure to DENV-1 and
567 DENV-4) vs. repeat detections within a serotype (e.g. detection of DENV-2 following prior
568 exposure to a previous lineage of DENV-2). The epidemic consequences of this invasion were
569 comparable, so long as enhanced detectability (e.g. antigenic escape) was specific to invading
570 lineage.

571

572 **DISCUSSION**

573 Drawing from two decades of national surveillance data and a more recent genomic
574 cohort study, we queried the mechanisms that underly dengue virus transmission and drive
575 periodic dengue epidemics in Cambodia. All told, our study highlights the complex interplay of
576 climate, demography, immunology, and virology that dictates the dynamics of dengue virus
577 disease in endemic settings.

578 Our investigations of climate effects on dengue transmission in Cambodia mirror those
579 previously reported in Thailand (28, 29), Sri Lanka (50), and China (46), emphasizing the role of
580 temperature, and—to a lesser extent—precipitation, in synchronizing annual dynamics in
581 epidemic years. Consistent with prior work that highlights a role for El Niño in driving multiannual
582 dengue cycles in other systems (29), we observed synchrony between reconstructed multiannual
583 dengue cycles in Cambodia and the ONI; however, this synchrony appeared to peak during the
584 robust 2015-2016 El Niño, which did not correspond to one of the three major dengue epidemic
585 years in our dataset—though some signature of elevated amplitude for multiannual dengue
586 cycles in northern Cambodia (adjacent to the Thai border) suggest a local epidemic may have

587 occurred during this time. The muted impact of climate on dengue dynamics in Cambodia could
588 reflect overall higher caseloads in association with elevated temperatures in more recent years
589 (28), making any further transmission gains comparatively less dramatic. In addition, climate
590 impacts on DENV transmission may be generally less discernable in Cambodia, which has
591 reduced latitudinal variation (and corresponding climate differences) than other SEA countries,
592 such as Thailand. Nonetheless, our analysis suggests that warmer temperatures play a role in
593 driving epidemic dynamics for Cambodian dengue and likely contributed to high caseloads in
594 2019. As temperatures increase globally, dengue transmission is likely to accelerate, and
595 variation in both timing of annual dengue transmission and multiannual peaks in caseload may
596 become more homogenous.

597 In addition to climate, our data and corresponding analysis emphasize the importance of
598 human demography and prior immunity in structuring dengue transmission globally. Consistent
599 with studies conducted elsewhere (23–25), we observed a pattern of increasing mean age of
600 reported dengue infection that we effectively recaptured by modeling a declining FOI through
601 time—which we attributed to declining birth and death rates consistent with Cambodia’s
602 demographic transition. Certainly, other mechanisms of demographic change (e.g. immigration
603 and emigration) could also impact infection dynamics. Cambodia experienced a net negative
604 migration rate across the time series investigated (61); as the majority of Cambodian migrants are
605 young adults seeking employment in neighboring Thailand (62), it is possible that their emigration
606 could lower the dengue FOI even further. Though the Cambodian migrant population comprises
607 <0.5% of the total national population (61), migration rates can be 10-fold higher in border
608 provinces and could have correspondingly elevated impacts in these regions (62).

609 The declining FOI through time is somewhat counterintuitive considering recent explosive
610 dengue epidemics in Cambodia and across the globe. Nonetheless, we provide evidence for a
611 high frequency of reported cases in older age individuals that underlies the high case burden in
612 epidemic years. Our study is unique from previous investigations in recognition, not only of
613 escalation of the mean age of reported dengue infection, but also of the expanding age range of

614 reported disease. Indeed, symptomatic individuals >70 years in age during the 2019 epidemic are
615 difficult to reconcile under assumptions by which reported cases correspond to clinically apparent
616 secondary infections only. In our modeling framework, we take a novel approach to account for
617 these infections by allowing for waning multitypic immunity and repeated symptomatic infections
618 in older age individuals.

619 Recent analyses out of the Thailand system highlight a similar uptick in case reports
620 among older individuals (23), which the authors attribute to increased detectability in tertiary and
621 quaternary infections. The authors offer a series of hypothetical explanations for increasing case
622 detectability through time: that tertiary and quaternary dengue infections might be more
623 pathogenic (and therefore more detectable) due to an abundance of comorbidities in older
624 individuals, that immunopathology may be exacerbated in older patients who experienced longer
625 durations between repeat infections; or that waning multitypic immunity could allow for repeat
626 infections in the oldest age cohorts (our hypothesis). Our analyses in the Cambodia system are
627 not mutually exclusive with any of these explanations; however, we hypothesize that, were
628 comorbidities or immunopathogenesis in older individuals driving patterns in the observed data,
629 we would expect to see an hour-glass shape in symptomatic cases, with reduced reporting in
630 middle-aged individuals who have progressed beyond secondary exposures but are at lower risk
631 for both comorbidities and immunopathology. Instead, we see a gradual tapering in the age-
632 frequency of infection, which expands in range with time (Fig. S15), consistent with the
633 hypothesis of waning multitypic immunity. This latter hypothesis, when considered in association
634 with genotype replacement, can also explain isolated expansion and subsequent contraction in
635 the age range of reported cases witnessed in epidemic years, while the first two hypotheses
636 cannot. In addition, hypotheses of heightened pathology in more frequent older age infections are
637 difficult to reconcile in Cambodia with nationally-reported declines in the dengue mortality burden
638 despite increasing caseload through time (15).

639 Our deterministic model simulations demonstrate how short-term spikes in the age
640 distribution of reported cases, independent of the mean annual trend in the time series, can be

641 achieved via introduction of an antigenically distinct lineage (either a divergent genotype within an
642 established serotype, or a novel serotype) into an endemic, 3-serotype system. Though limited in
643 scope, PCR-based sentinel surveillance data provide no support for serotype turnover associated
644 with the 2019 dengue epidemic in Cambodia (15). By contrast, genome sequencing data from our
645 own febrile cohort study offer support for a genotype replacement event. Recent analyses of the
646 Thailand system link transitions in serotype dominance and clade replacement of genotype
647 sublineages within a single serotype to epidemic magnitude (34, 35). In Thailand, the most
648 severe epidemics were linked to clade replacement of a resident viral genotype by an
649 evolutionarily fitter DENV lineage within the same serotype, resulting in a 'selective sweep', which
650 subsequently reduced overall viral diversity and, consequently, diminished between-serotype
651 antigenic differences (34). In the 2019 epidemic in Cambodia, emergence of the Cosmopolitan
652 genotype, followed by serotypic and genotypic homogeneity in 2020-2022, are consistent with the
653 dynamics of clade replacement within DENV-2. Indeed, prior clade replacements have been
654 associated with epidemics in Cambodia (17, 18) and elsewhere (50, 54, 63–65).

655 As one limitation of our study, the bulk of our genotyping efforts were concentrated in
656 peri-urban Kampong Speu province, allowing for the possibility that the clade replacement
657 phenomenon documented here may be regionally localized, with consequentially limited impacts
658 on national caseloads. Nonetheless, the predominance of the DENV-2 Genotype-V lineage in the
659 mid-2000s has been well-documented across most provinces in Cambodia (66, 67), and our
660 extended sequencing efforts in 2021-2022 suggest that the Cosmopolitan (Genotype-II) takeover
661 covered a similarly widespread geographic extent. Additionally, reemergence of DENV-2
662 Cosmopolitan lineage has also been documented in neighboring Vietnam and associated with a
663 2019 epidemic (53), suggesting a more generalized regional phenomenon.

664 Our study faces additional limitations in that we were unable to obtain virus isolates and
665 undertake subsequent antigenic cartography (68), which would be needed to resolve whether the
666 emerging Cosmopolitan genotype (Genotype-II) in Cambodia is, indeed, antigenically distinct
667 from previously circulating Genotype-V lineages of DENV-2 and, potentially, more antigenically

668 similar to endemic heterotypic viruses. Indeed, because much of our inference is derived from
669 serotype-agnostic national surveillance data, we are unable to rigorously evaluate the role of a
670 possible genotype replacement event in particularly driving a high burden of disease in the oldest-
671 age (>70 years) individuals in NDCP dataset. Nonetheless, the expansion of this lineage
672 following the 2019 epidemic suggests some enhanced fitness for this genotype in our setting—
673 though, whether mediated by increased transmissibility, immune escape, or both, is difficult to
674 say. Our own febrile surveillance study demonstrates a significantly older mean age of infection
675 for DENV-2 Cosmopolitan cases than for DENV-1 cases, which supports a hypothesis of invasion
676 paired with immune escape. Critically, our simulation analyses demonstrate how the expanded
677 age distribution of cases witnessed across epidemic years in Cambodia can only be recovered
678 under assumptions of invasion or expansion with lineage-specific waning immunity.

679 Several published studies offer regional explanations for the global dengue phenomenon
680 of 2019. Recent analyses from Brazil, for example, argue that a low FOI in 2017 and 2018
681 resulting from new public health interventions and behavioral modifications implemented in the
682 wake of the Zika virus epidemic drove a resurgence in cases in 2019 and an expansion of
683 specific lineages of DENV-1 and DENV-2 that had been circulating cryptically for much of the
684 past decade (69). Independent work in the same region indicates that the DENV-2 lineage
685 responsible for the Brazilian outbreak additionally caused a clade replacement event (64).
686 Dengue surged worldwide in 2019, though the factors driving this surge appear to be somewhat
687 heterogenous across ecosystems. Nonetheless, our study lends support for the role of climate in
688 synchronizing epidemic dynamics across landscapes; it is possible that optimal climate conditions
689 may facilitate expansion of low prevalence lineages with intrinsic fitness advantages (e.g. higher
690 replication rate, shorter incubation period (70)) over resident genotypes, thus driving epidemics.
691 Previous modeling studies have suggested that invading dengue lineages may circulate at low
692 prevalence in a host population for many years prior to detection, expansion, and displacement of
693 resident clades in the same serotype (71).

694 Here, we propose the emergence of the DENV-2 Cosmopolitan genotype (Genotype-II),
695 coupled with a subtle climate-driven increase in FOI, and overlaid on the background of an aging
696 population with waning multitypic immunity, as one possible explanation for Cambodia's largest
697 recorded dengue epidemic to date. Our study emphasizes the extraordinary dearth of publicly
698 available DENV sequence data for SEA; indeed, DENV is sequenced so infrequently in
699 Cambodia that it is impossible to know whether 2019 truly marked the first year of DENV-2
700 Cosmopolitan introduction to the country, or simply the year of intensified expansion and
701 consequential epidemic dynamics. More broadly, our work illustrates the importance of the
702 combined forces of climate, demography, immunology, and virology in driving increasingly severe
703 dengue epidemics. As the global burden of dengue continues to expand, ongoing serological and
704 genomic surveillance is needed to improve epidemic forecasting in Southeast Asia and around
705 the world.

706

707

708

709 **METHODS**

710

711 *Data*

712 Detailed descriptions of NDCP case data, climate data, and Kampong Speu febrile
713 surveillance data used in these analyses are reported in the *SI Appendix*.

714

715 *Climate analyses*

716 We used GAMs to quantify intra- and interannual trends and identify any years that might
717 be considered climatic anomalies, defined as a statistically significant partial effect of a single
718 year on the long-term time series for temperature and precipitation (Fig. S1-4; Table S1; *SI*
719 *Appendix*). In addition, we reduced temperature and precipitation time series by province into z-
720 scores for visualization (Fig. S5-6).

721 *Climate-informed TSIR modeling*

722 Using the R package tSIR (43), we fit time series Susceptible-Infected-Recovered models
723 (43–45) to the province level dengue data for the three inter-epidemic periods (2002–2006, 2008–
724 2011, and 2013–2018), compiled at biweekly intervals corresponding to the generation time of the
725 pathogen (*SI Appendix*). Using TSIR transmission parameters, we projected cases in subsequent
726 epidemic years (2007, 2012, 2019) by province. We then followed Wagner et al. 2020 (50) to
727 estimate the factorial increase in reconstructed susceptible population needed to recover case
728 counts for the three epidemic years.

729 We next used cross correlation analysis to determine the optimal lag between biweekly
730 mean temperature and total precipitation versus transmission at the province level; we estimated
731 a median 3.5 month lag for temperature and 1 month lag for precipitation, consistent with prior
732 analyses (Table S3; *SI Appendix*) (50). We then constructed a suite of regression models
733 (including GAMs) for each interepidemic period, incorporating a response variable of the log of
734 biweekly transmission with the corresponding predictors of optimally lagged biweekly mean
735 temperature and total precipitation per province (46, 50) (Fig. S8–10; Table S4). We used lagged
736 temperature and precipitation from each epidemic year in each province in a fitted GAM to project
737 climate-informed transmission rates for 2007, 2012, and 2019 (*SI Appendix*). We then simulated
738 TSIR using climate-informed transmission rates to recover epidemic year predictions of province-
739 level caseload. Because climate-derived transmission rates still failed to recover epidemic peaks,
740 we allowed another susceptible amplification term to determine the relative increase in
741 susceptible population needed to recover epidemic dynamics even after accounting for climate
742 (Table S5).

743

744 *Wavelet analyses*

745 We next used wavelet decomposition in the R package ‘WaveletComp’ (51) to explore
746 annual and multiannual periodicity in dengue epidemics and climate variables. We converted
747 biweekly case totals by province from the NDCP data into incidence rates per 100,000

748 population, then used a Morlet wavelet with nondimensional frequency ($\omega = 6$) to extract,
749 detrend, and reconstruct annual cycles in dengue incidence with a maximum period of two years
750 and multiannual cycles with periods ranging from two to 20 years (Fig. 2AB) (28, 29). We
751 additionally calculated the average wavelet power (squared amplitude, here averaged across all
752 significant wavelets within a specified timestep) for significant cycles within each biweekly
753 timestep for annual and multiannual cycles per province (Fig. S11AB).

754 We investigated synchronicity in dengue incidence across space by computing the
755 Pearson's correlation coefficient (ρ) and the mean cross-wavelet power spectrum between
756 province pairs, using the annual raw incidence and reconstructed annual and multiannual cycles
757 (the latter averaged over a sliding 5-year interval) (Fig. 2CD, S11CD; *SI Appendix*). We
758 constructed a GAM to identify statistical correlates of high synchronicity pairs (Fig. S12; Table S6;
759 *SI Appendix*). To investigate synchrony between dengue and climate, we computed mean cross-
760 wavelet power between biweekly dengue incidence and mean temperature (Fig. S13A) and total
761 precipitation (Fig. S13B) per province, then repeated between reconstructed multiannual dengue
762 cycles over a 5-year interval and the same two climate variables, again per province (Fig.
763 S13CD). Finally, we reconstructed *monthly* multiannual dengue cycles per province to compute
764 average cross-wavelet power with the Oceanic Niño Index (ONI), a time series quantifying the
765 intensity of the El Niño Southern Oscillation (Fig. S13E). Lastly, we extracted the mean period
766 from reconstructed multiannual dengue cycles by province and nationally, to compare with
767 demographic data (birth rates, death rates, population size (61)) (Fig. S14).

768

769 *Increasing age of reported infection and FOI estimation*

770 To quantify interannual trends in the mean age of reported DENV infection, we fit a GAM
771 with a response variable of age to a fixed predictor of the interaction of year and province, with a
772 random effect of province, allowing both slope and y-intercept to vary by locality. We visualized
773 trends across the age distribution of reported cases by province (Fig. S15) and summarized
774 nationally (Fig. 3AB; Table S7).

775 To estimate annual FOI for DENV in Cambodia from 2002-2020, we applied the model
776 developed by Ferguson et al. 1999 (36) and Cummings et al. 2009 (24) to age-structured
777 incidence recovered from the NDCP data, at the province level, assuming reported cases to
778 represent secondary infections and individuals in the dataset to experience exposure to multiple
779 DENV serotypes across their lifetimes. We allowed for a unique FOI across each year in the time
780 series but first assumed constant FOI across all age cohorts within a year. We estimated one FOI
781 per year per province (excepting Tboung Khmum), in addition to a summary national FOI, for all
782 years in the dataset and extending back to the year of birth for the oldest individual in the first
783 year of the corresponding data subset (40 years for national data) (Fig. S16; Table S8; *SI*
784 *Appendix*). We estimated mean FOI per serotype assuming four circulating dengue serotypes
785 and plotted FOI estimates in comparison to national reported birth and death rates (Fig. 3C) (61).

786 After fixing FOI by province, we followed prior work (24) to estimate FOI modifiers by age,
787 shared across all provinces. We fit nineteen age-specific modifiers to the fixed FOI values,
788 corresponding to eight age classes in first decade of the dataset and eleven in the second
789 decade, where the age distribution was larger (Table S8). We then modified our model to allow
790 waning from multitypic back to monotypic immunity (σ), such that older individuals could
791 experience renewed symptomatic infections (*SI Appendix*). As with age-modification terms, we
792 estimated waning multitypic immunity shared across all provinces but allowed σ to vary annually.
793 We compared fits of FOI-only, FOI with age modification, FOI with waning multitypic immunity,
794 and FOI with both age modification and waning multitypic immunity models to the data (Table
795 S8), then simulated the resulting accumulation of cases with age from the best fit model at
796 national (Fig. 3E) and province levels (Fig. S17).

797

798 *Viral sequencing*

799 mNGS was applied to RNA extracted from 239 serum samples collected from patients
800 reporting with symptoms in our 2019-2022 febrile cohort study in Kampong Speu province, with
801 an additional subset of 11 samples sourced from five nearby provinces (40). A further 20 samples

802 were received for RNA extraction and mNGS from six provinces (including 8 from Kampong
803 Speu) in part with 2021-2022 NDCP surveillance (Table S9; Fig. 4AB). See *SI Appendix* for
804 detailed methods for library preparation, sequencing, and consensus genome generation. We
805 successfully generated 192 full or near-full genome sequences from the original 270 samples,
806 which we submitted to NCBI (63 DENV-1, 120 DENV-2, and 9 DENV-4). All contributed genomes
807 were >10,000 bps in length and had a maximum of 90 Ns (corresponding to <1% of the DENV
808 genome). Samples for which full genome recovery was not possible were identified to genotype
809 using BLAST (72) and visualized in Fig. 4AB (Table S9).

810

811 *Phylodynamic and phylogenetic analysis*

812 See *SI Appendix* for details of sequence selection for Bayesian phylodynamic timetrees
813 and maximum likelihood phylogenies. After selection, sequences were aligned by serotype in the
814 program MAFFT (73), and the best fit nucleotide substitution model for each serotype was
815 evaluated in ModelTest-NG (74). Using the best-fit model (GTR+I+G4 in all cases), we built a
816 Bayesian phylogenetic tree for each serotype in BEAST 2 (57), incorporating the date of sample
817 collection for each sequence (or the midpoint of the collection year if date was not reported), and
818 specifying a strict molecular clock rate of 7.9×10^{-4} s/s/y (8) and a Coalescent Bayesian skyline
819 prior. We ran Markov Chain Monte Carlo chains for 150 million iterations, logging results every
820 10,000 iterations. After chains completed, we removed the initial 10% of iterations as burn-in and
821 evaluated parameter convergence ($ESS \geq 200$) in Tracer v1.6. We summarized resulting
822 phylogenetic trees in TreeAnnotator and visualized summary trees in ggtrree (75) (Fig. 4CD; Fig.
823 S18, S19). Serotype-specific maximum likelihood phylogenetic trees were constructed in RAxML
824 (76). Twenty ML inferences were made on each original alignment and bootstrap replicate trees
825 were inferred using Felsenstein's method (77), with the MRE-based bootstrapping test applied
826 after every 50 replicates (78). Resulting phylogenies were visualized in ggtrree (75) (Fig. S18).

827 We followed Salje et al. 2017 (8) to calculate the proportion of sequences within each
828 DENV serotype that could be attributed to the same transmission chain on our Bayesian

829 timetrees, defined as having an MRCA within the past six months in the same season (see Fig.
830 S20 for alternative MRCA cutoffs). We compared the proportion of DENV-1 vs. DENV-2
831 sequences sharing a transmission chain to the Euclidean distance separating the GPS
832 coordinates for each sequence pair (Fig. 4E). We then computed the total effective number of
833 transmission chains (the reciprocal of the proportion of sequences sharing a chain) in our 2019-
834 2022 Kampong Speu sequence dataset for DENV-1 and DENV-2 at the World Bank reported
835 population density for Kampong Speu province (61) (Fig. 4F).

836

837 *Mechanistic modeling of age-structured dengue dynamics*

838 Finally, we constructed a mechanistic, age-structured discrete time deterministic model in
839 biweekly timesteps (58–60) to simulate three-serotype dengue dynamics in a population
840 demographically structured to mimic that of Cambodia over the past half-century (*SI Appendix*).
841 We compared simulations under (H0) baseline demographic assumptions with simulations of (H1)
842 increasing tertiary case detections through time and (H2) genotype invasion and clade-
843 replacement with waning immunity, timed both in 2019 and in 2007. We additionally simulated
844 novel genotype invasions under (H3) assumptions of no antigenic escape, or (H4) lineage-
845 agnostic increasing tertiary case detection (Fig. S21). Finally, we fit the Ferguson-Cummings
846 four-serotype catalytic model to the simulated data for each hypothesis to recapture the input FOI
847 (Fig. S22). Holding FOI constant, we estimated a time-varying signature of waning monotypic
848 immunity for all simulated time series (Fig. S22).

849

850 **ACKNOWLEDGEMENTS**

851 This research is supported by the Division of Intramural Research at the National Institute
852 of Allergy and Infectious Diseases at the National Institutes of Health and the Bill and Melinda
853 Gates Foundation [OPP1211806, OPP1211841]. We thank patients and families of Kampong
854 Speu District Referral Hospital who participated in this study, members of the National Dengue
855 Control Program not listed in the author byline, and the Provincial Health Department of Kampong

856 Speu province in Cambodia. We thank Brian Moyer and the NIAID Office of Cyberinfrastructure
857 and Computational Biology (OCICB) for assistance in improving the cyberinfrastructure of our
858 Cambodian field sites. We thank employees at the Chan Zuckerberg Biohub and Chan
859 Zuckerberg Initiative not listed in the author byline. This work was completed with resources
860 provided by the University of Chicago Research Computing Center.

861

862

863

864

865

866

867

868

869

870

871

872

873

874

875

876

877

878

879

880

881

882

883 **REFERENCES**

- 884 1. World Health Organization, Dengue and severe dengue. *WHO Fact Sheets* (2022).
- 885 2. S. Bhatt, *et al.*, The global distribution and burden of dengue. *Nature* **496**, 504–507 (2013).
- 886 3. A. B. Sabin, Research on dengue during World War II. *American Journal of Tropical*
887 *Medicine and Hygiene* **1**, 30–50 (1952).
- 888 4. L. C. Katzelnick, *et al.*, Antibody-dependent enhancement of severe dengue disease in
889 humans. *Science (New York, N.Y.)* **932**, 929–932 (2017).
- 890 5. L. C. Katzelnick, *et al.*, Zika virus infection enhances future risk of severe dengue disease.
891 *Science* **369**, 1123–1128 (2020).
- 892 6. T. N. Peng, “Southeast Asia’s demographic situation, regional variations, and national
893 challenges” in D. Singh, M. Cook, Eds. (ISEAS Publishing, 2017), pp. 55–82.
- 894 7. G. W. Jones, “The Population of Southeast Asia” (2013).
- 895 8. H. Salje, *et al.*, Dengue diversity across spatial and temporal scales: Local structure and the
896 effect of host population size. *Science (New York, N.Y.)* **355**, 1302–1306 (2017).
- 897 9. statista, Cambodia: Urbanization from 2010 to 2020.
898 <https://www.statista.com/statistics/455789/urbanization-in-cambodia/>. (2022).
- 899 10. J. H. Huber, M. L. Childs, J. M. Caldwell, E. A. Mordecai, Seasonal temperature variation
900 influences climate suitability for dengue, chikungunya, and Zika transmission. *PLoS Negl*
901 *Trop Dis* **12**, e0006451 (2018).
- 902 11. E. A. Gould, S. Higgs, Impact of climate change and other factors on emerging arbovirus
903 diseases. *Transactions of the Royal Society of Tropical Medicine and Hygiene* **103**, 109–121
904 (2009).
- 905 12. J. P. Messina, *et al.*, The current and future global distribution and population at risk of
906 dengue. *Nature Microbiology* **4**, 1508–1515 (2019).
- 907 13. Hahn, H., Chastel, C., Dengue in Cambodia in 1963. Nineteen laboratory-proved cases.
908 *American Journal of Tropical Medicine and Hygiene* **19**, 106–109 (1970).
- 909 14. R. Huy, *et al.*, National dengue surveillance in Cambodia 1980–2008: epidemiological and
910 virological trends and the impact of vector control. *Bull. World Health Organ.* **88**, 650–657
911 (2010).
- 912 15. C. Yek, *et al.*, National dengue surveillance, Cambodia 2002–2020. *Bull World Health Org*
913 **101**, 605–616 (2023).

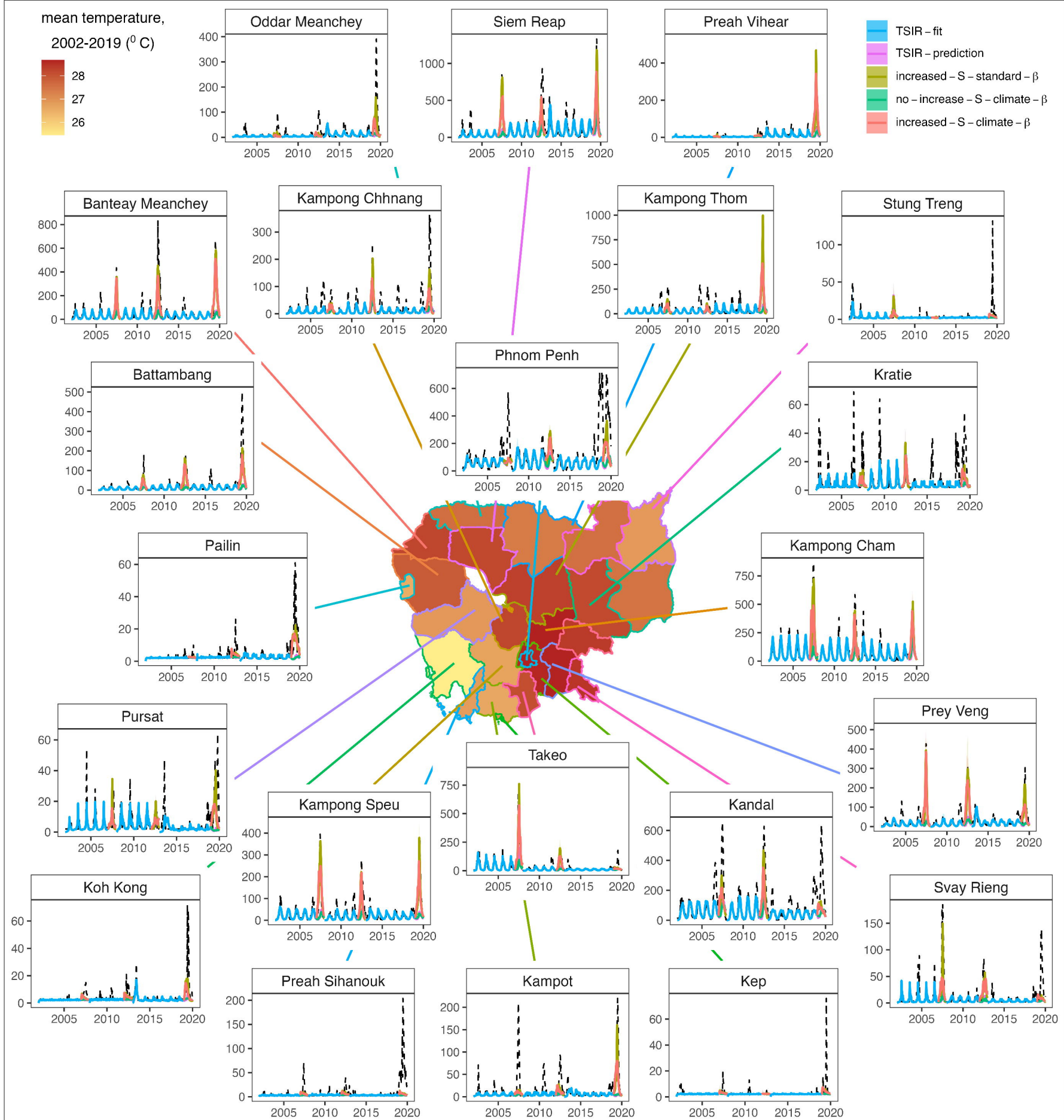
- 914 16. D. S. Burke, A. Nisalak, D. E. Johnson, A prospective study of dengue infections in Bangkok.
915 *The American Journal of Tropical Medicine and Hygiene* **38**, 172–180 (1988).
- 916 17. V. Duong, *et al.*, Genetic diversity and lineage dynamic of dengue virus serotype 1 (DENV-
917 1) in Cambodia. *Infection, Genetics and Evolution* **15**, 59–68 (2013).
- 918 18. O. O'Connor, *et al.*, Potential role of vector-mediated natural selection in dengue virus
919 genotype/lineage replacements in two epidemiologically contrasted settings. *Emerging
920 Microbes and Infections* **10**, 1346–1357 (2021).
- 921 19. A. A. Lover, *et al.*, Spatial epidemiology and climatic predictors of paediatric dengue
922 infections captured via sentinel site surveillance, Phnom Penh Cambodia 2011-2012. *BMC
923 Public Health* **14** (2014).
- 924 20. Y. Arima, M. Chiew, T. Matsui, Epidemiological update on the dengue situation in the
925 Western Pacific Region, 2012. *Western Pacific surveillance and response journal : WPSAR*
926 **6**, 82–89 (2015).
- 927 21. S. Ly, *et al.*, Asymptomatic dengue virus infections, Cambodia, 2012–2013. *Emerging
928 Infectious Diseases* **25**, 1354–1362 (2019).
- 929 22. S. Vong, *et al.*, Under-recognition and reporting of dengue in Cambodia: A capture-
930 recapture analysis of the National Dengue Surveillance System. *Epidemiology and Infection*
931 **140**, 491–499 (2012).
- 932 23. A. T. Huang, *et al.*, Assessing the role of multiple mechanisms increasing the age of dengue
933 cases in Thailand. *Proc. Natl. Acad. Sci. U.S.A.* **119**, e2115790119 (2022).
- 934 24. D. A. T. Cummings, *et al.*, The impact of the demographic transition on dengue in Thailand:
935 Insights from a statistical analysis and mathematical modeling. *PLoS Medicine* **6** (2009).
- 936 25. L. C. Katzelnick, *et al.*, Dynamics and determinants of the force of infection of dengue virus
937 from 1994 to 2015 in Managua, Nicaragua. *Proceedings of the National Academy of
938 Sciences of the United States of America* **115**, 10762–10767 (2018).
- 939 26. N. Ferguson, R. Anderson, S. Gupta, The effect of antibody-dependent enhancement on
940 the transmission dynamics and persistence of multiple-strain pathogens. *Proc. Natl. Acad.
941 Sci. U.S.A.* **96**, 790–794 (1999).
- 942 27. S. I. Hay, *et al.*, Etiology of interepidemic periods of mosquito-borne disease. *Proc. Natl.
943 Acad. Sci. U.S.A.* **97**, 9335–9339 (2000).
- 944 28. B. García-Carreras, *et al.*, Periodic synchronisation of dengue epidemics in Thailand over
945 the last 5 decades driven by temperature and immunity. *PLoS Biol* **20**, e3001160 (2022).
- 946 29. W. G. van Panhuis, *et al.*, Region-wide synchrony and traveling waves of dengue across
947 eight countries in Southeast Asia. *Proc. Natl. Acad. Sci. U.S.A.* **112**, 13069–13074 (2015).

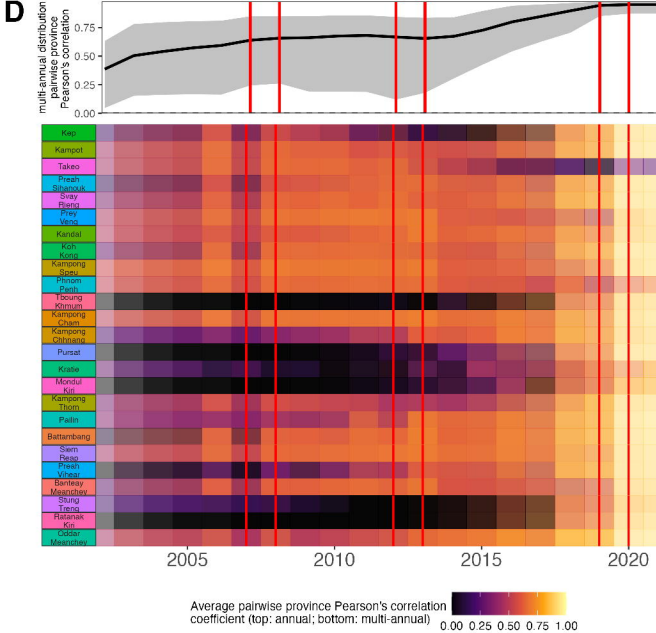
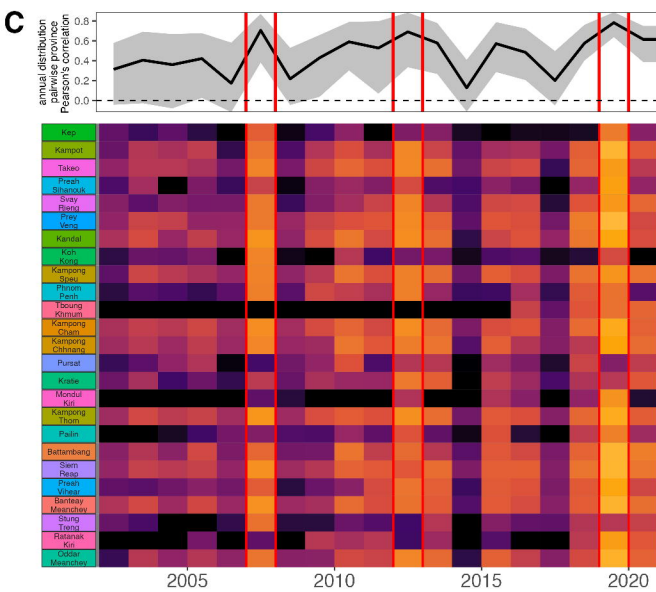
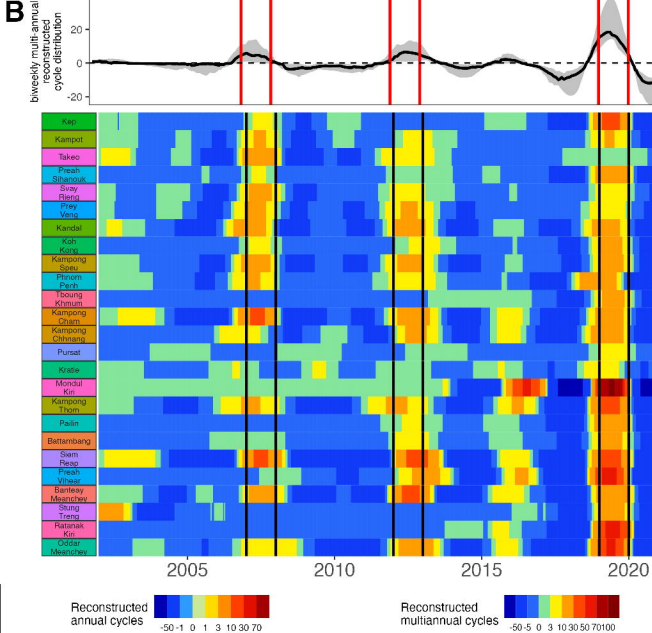
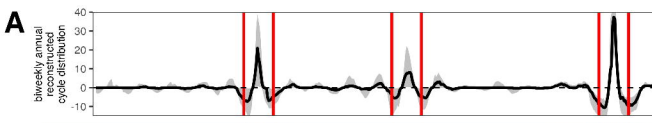
- 948 30. D. A. T. Cummings, I. B. Schwartz, L. Billings, L. B. Shaw, D. S. Burke, Dynamic effects of
949 antibody-dependent enhancement on the fitness of viruses. *Proceedings of the National
950 Academy of Sciences* **102**, 15259–15264 (2005).
- 951 31. K. L. McElroy, *et al.*, Endurance, refuge, and reemergence of dengue virus type 2, Puerto
952 Rico, 1986–2007. *Emerg. Infect. Dis.* **17**, 64–71 (2011).
- 953 32. B. Adams, *et al.*, Cross-protective immunity can account for the alternating epidemic
954 pattern of dengue virus serotypes circulating in Bangkok. *Proceedings of the National
955 Academy of Sciences of the United States of America* **103**, 14234–9 (2006).
- 956 33. C. V. F. Carrington, J. E. Foster, O. G. Pybus, S. N. Bennett, E. C. Holmes, Invasion and
957 maintenance of Dengue virus type 2 and type 4 in the Americas. *Journal of Virology* **79**,
958 14680–14687 (2005).
- 959 34. L. C. Katzelnick, *et al.*, Antigenic evolution of dengue viruses over 20 years. *Science* (2021).
- 960 35. S. M. Bell, L. Katzelnick, T. Bedford, Dengue genetic divergence generates within-serotype
961 antigenic variation, but serotypes dominate evolutionary dynamics. *eLife* **8**, e42496 (2019).
- 962 36. N. M. Ferguson, C. A. Donnelly, R. M. Anderson, Transmission dynamics and epidemiology
963 of dengue: insights from age-stratified sero-prevalence surveys. *Proceedings of the Royal
964 Society B* **354**, 757–768 (1999).
- 965 37. Hugo. Muench, *Catalytic models in epidemiology*. (Harvard University Press, 1959).
- 966 38. J. E. Manning, *et al.*, Development of inapparent dengue associated with increased
967 antibody levels to *Aedes aegypti* salivary proteins: A longitudinal dengue cohort in
968 Cambodia. *The Journal of Infectious Diseases* (2021).
969 <https://doi.org/10.1093/infdis/jiab541>.
- 970 39. V. Fonseca, *et al.*, A computational method for the identification of Dengue, Zika and
971 Chikungunya virus species and genotypes. *PLoS Negl Trop Dis* **13**, e0007231 (2019).
- 972 40. J. A. Bohl, *et al.*, Discovering disease-causing pathogens in resource-scarce Southeast Asia
973 using a global metagenomic pathogen monitoring system. *Proceedings of the National
974 Academy of Sciences* **119**, e2115285119 (2022).
- 975 41. S. N. Wood, mgcv: GAMs and Generalized Ridge Regression for R. *R News* **1/2**, 20–24
976 (2001).
- 977 42. NOAA: National Weather Service, *Climate Predication Scenter: Cold & Warm Episodes by
978 Season* (2023). Available at:
979 https://origin.cpc.ncep.noaa.gov/products/analysis_monitoring/ensostuff/ONI_v5.php.
- 980 43. A. D. Becker, B. T. Grenfell, TSIR: An R package for time-series susceptible-infected-
981 recovered models of epidemics. *PLoS ONE* **12**, 1–10 (2017).

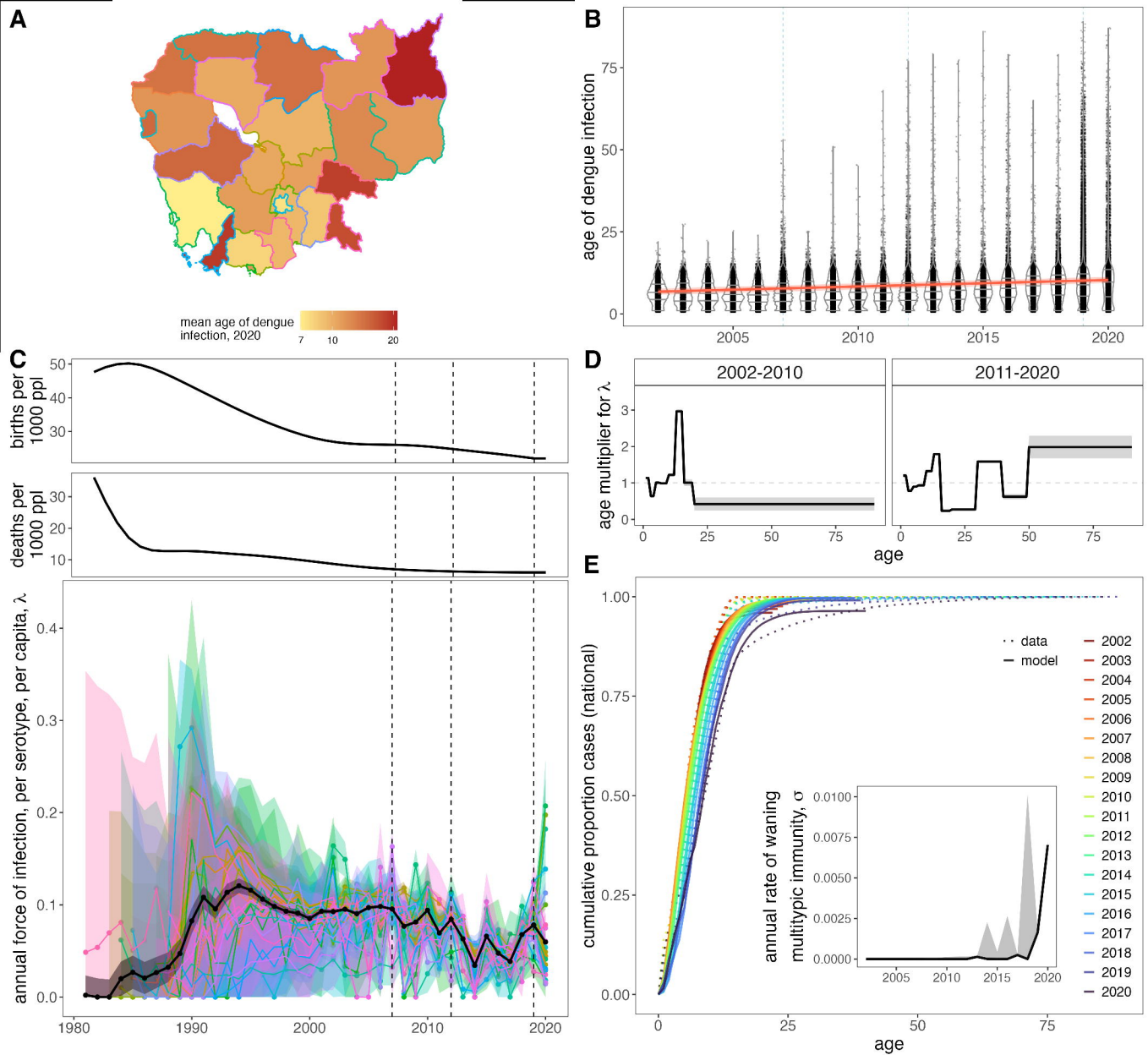
- 982 44. O. N. Bjornstad, B. F. Finkenstadt, B. T. Grenfell, Dynamics of measles epidemics:
983 Estimating scaling of transmission rates using a times series SIR model. *Ecological*
984 *Monographs* **72**, 169–184 (2002).
- 985 45. B. T. Grenfell, O. N. Bjornstad, B. F. Finkenstadt, Dynamics of measles epidemics: Scaling
986 noise, determinism, and predictability with the TSIR Model. *Ecological Monographs* **72**,
987 185–202 (2002).
- 988 46. R. J. Oidtmann, *et al.*, Inter-annual variation in seasonal dengue epidemics driven by
989 multiple interacting factors in Guangzhou, China. *Nature Communications* **10** (2019).
- 990 47. N. A. Rehman, *et al.*, Quantifying the localized relationship between vector containment
991 activities and dengue incidence in a real-world setting: A spatial and time series modelling
992 analysis based on geo-located data from Pakistan. *PLoS Neglected Tropical Diseases* **14**, 1–
993 22 (2020).
- 994 48. M. U. G. Kraemer, *et al.*, Big city, small world: density, contact rates, and transmission of
995 dengue across Pakistan. *J. R. Soc. Interface* **12**, 20150468 (2015).
- 996 49. M. U. G. Kraemer, *et al.*, Inferences about spatiotemporal variation in dengue virus
997 transmission are sensitive to assumptions about human mobility: a case study using
998 geolocated tweets from Lahore, Pakistan. *EPJ Data Science* **7** (2018).
- 999 50. C. E. Wagner, *et al.*, Climatological, virological and sociological drivers of current and
1000 projected dengue fever outbreak dynamics in Sri Lanka. *Journal of the Royal Society*
1001 *Interface* **17** (2020).
- 1002 51. Roesch, Angi, Schmidbauer, Harald, WaveletComp: Computational Wavelet Analysis. R
1003 package version 1.1. (2018). Deposited 2018.
- 1004 52. J. Phadungsombat, *et al.*, Emergence of genotype cosmopolitan of dengue virus type 2 and
1005 genotype III of dengue virus type 3 in Thailand. *PLoS ONE* **13**, 1–26 (2018).
- 1006 53. V. T. Tran, *et al.*, Reemergence of Cosmopolitan genotype dengue virus serotype 2,
1007 southern Vietnam. *Emerg. Infect. Dis.* **29** (2023).
- 1008 54. A. Wijewickrama, *et al.*, Emergence of a Dengue virus serotype 2 causing the largest ever
1009 dengue epidemic in Sri Lanka. *bioRxiv* (2018). <https://doi.org/10.1101/329318>.
- 1010 55. H. A. Tissera, *et al.*, Severe dengue epidemic, Sri Lanka, 2017. *Emerg. Infect. Dis.* **26**, 682–
1011 691 (2020).
- 1012 56. A. J. Drummond, M. A. Suchard, D. Xie, A. Rambaut, Bayesian phylogenetics with BEAUTi
1013 and the BEAST 1.7. *Molecular Biology and Evolution* **29**, 1969–1973 (2012).
- 1014 57. R. Bouckaert, *et al.*, BEAST 2: A software platform for Bayesian evolutionary analysis. *PLoS*
1015 *Computational Biology* **10** (2014).

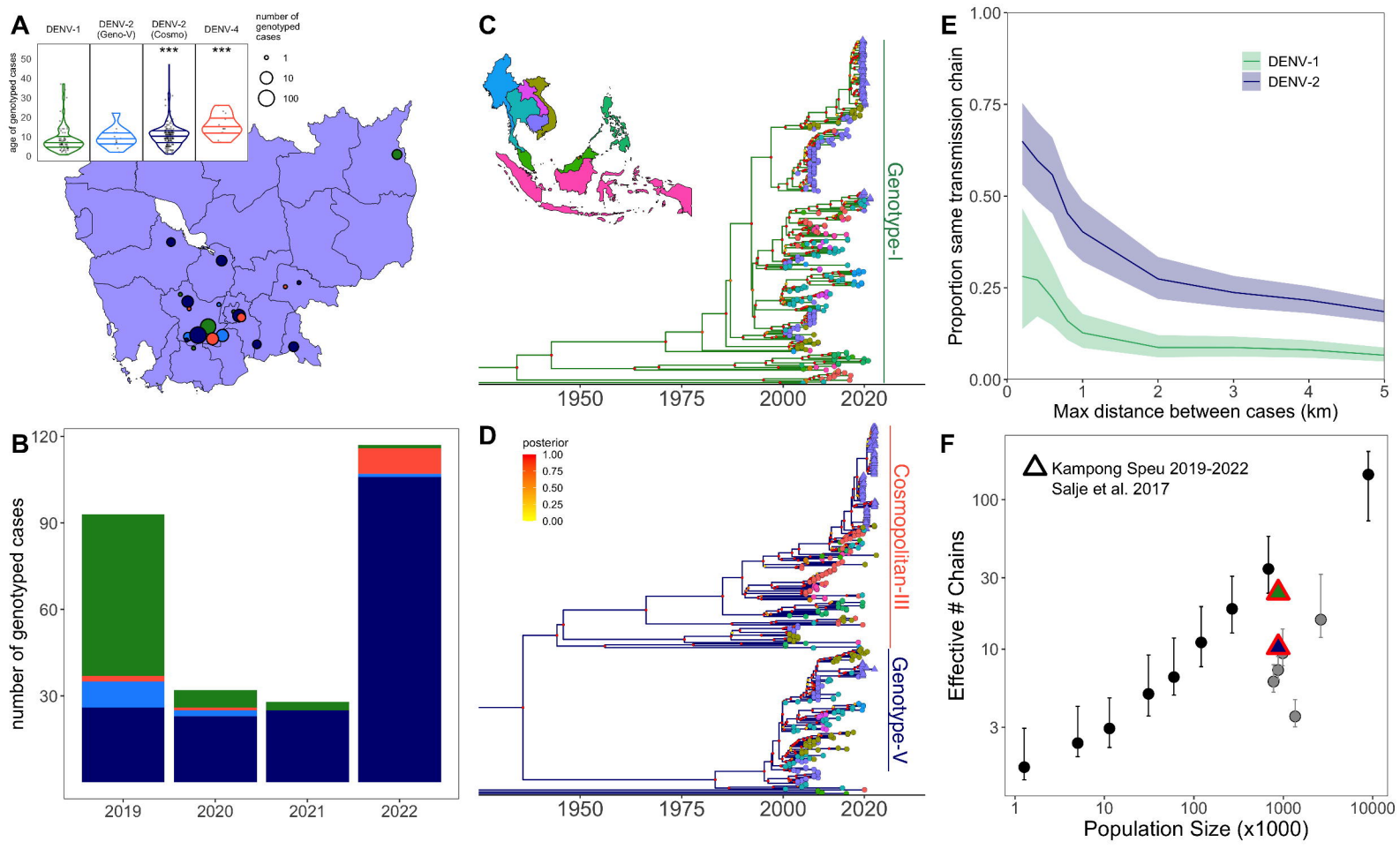
- 1016 58. P. Klepac, H. Caswell, The stage-structured epidemic: Linking disease and demography with
1017 a multi-state matrix approach model. *Theoretical Ecology* **4**, 301–319 (2011).
- 1018 59. C. J. E. Metcalf, *et al.*, Structured models of infectious disease: Inference with discrete
1019 data. *Theoretical Population Biology* **82**, 275–282 (2012).
- 1020 60. P. Klepac, *et al.*, Stage-structured transmission of phocine distemper virus in the Dutch
1021 2002 outbreak. *Proceedings. Biological sciences / The Royal Society* **276**, 2469–2476
1022 (2009).
- 1023 61. World Bank, Cambodia. *World Development Indicators* (2021). Available at:
1024 <https://data.worldbank.org/country/KH> [Accessed 12 April 2022].
- 1025 62. I. A. Sampson, G. M. Miles, E. Piano, “Undocumented, unregistered and invisible”: an
1026 exploratory study of the reasons for and effects of migrating to Thailand of Cambodian
1027 young people. *IJSSP* **41**, 862–874 (2021).
- 1028 63. L. Lambrechts, *et al.*, Dengue-1 virus clade replacement in Thailand associated with
1029 enhanced mosquito transmission. *Journal of Virology* **86**, 1853–1861 (2012).
- 1030 64. J. G. de Jesus, *et al.*, Genomic detection of a virus lineage replacement event of dengue
1031 virus serotype 2 in Brazil, 2019. *Memorias do Instituto Oswaldo Cruz* **115** (2020).
- 1032 65. K. Suzuki, *et al.*, Genotype replacement of dengue virus type 3 and clade replacement of
1033 dengue virus type 2 genotype Cosmopolitan in Dhaka, Bangladesh in 2017. *Infection,
1034 Genetics and Evolution* **75** (2019).
- 1035 66. V. Duong, *et al.*, Complex dynamic of dengue virus serotypes 2 and 3 in Cambodia
1036 following series of climate disasters. *Infection, Genetics and Evolution* **15**, 77–86 (2013).
- 1037 67. V. T. T. Hang, *et al.*, Emergence of the Asian 1 genotype of dengue Virus serotype 2 in Viet
1038 Nam: *In Vivo* fitness advantage and lineage replacement in South-East Asia. *PLoS
1039 Neglected Tropical Diseases* **4** (2010).
- 1040 68. L. C. Katzelnick, *et al.*, Dengue viruses cluster antigenically but not as discrete serotypes.
1041 *Science* **349**, 1338–1343 (2015).
- 1042 69. A. F. Brito, *et al.*, Lying in wait: the resurgence of dengue virus after the Zika epidemic in
1043 Brazil. *Nature Communications* **12**, 1–13 (2021).
- 1044 70. R. Rico-Hesse, *et al.*, Origins of Dengue type 2 viruses associated with increased
1045 pathogenicity in the Americas. *Virology* **230**, 244–251 (1997).
- 1046 71. J. Lourenço, M. Recker, Viral and epidemiological determinants of the invasion dynamics of
1047 Novel Dengue Genotypes. *PLoS Neglected Tropical Diseases* **4** (2010).
- 1048 72. S. F. Altschul, W. Gish, W. Miller, E. W. Myers, D. J. Lipman, Basic local alignment search
1049 tool. *Journal of Molecular Biology* **215**, 403–410 (1990).

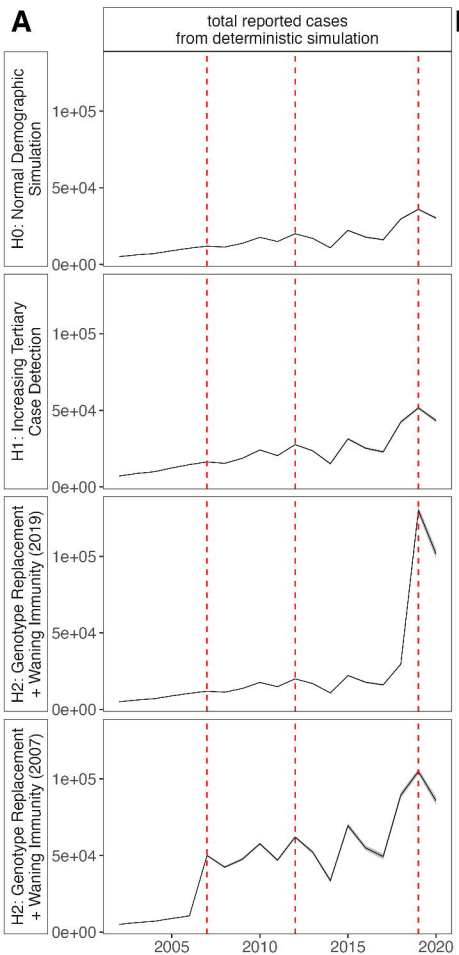
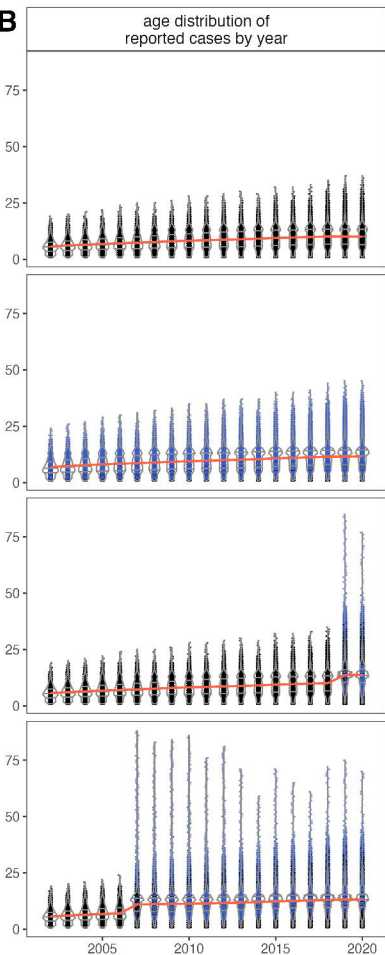
- 1050 73. K. Katoh, J. Rozewicki, K. D. Yamada, MAFFT online service: Multiple sequence alignment,
1051 interactive sequence choice and visualization. *Briefings in Bioinformatics* **20**, 1160–1166
1052 (2018).
- 1053 74. Di. Darriba, *et al.*, ModelTest-NG: A new and scalable tool for the selection of DNA and
1054 protein evolutionary models. *Molecular Biology and Evolution* **37**, 291–294 (2020).
- 1055 75. G. Yu, D. K. Smith, H. Zhu, Y. Guan, T. T. Y. Lam, Ggtree: an R Package for visualization and
1056 annotation of phylogenetic trees with their covariates and other associated data. *Methods*
1057 in *Ecology and Evolution* **8**, 28–36 (2017).
- 1058 76. A. M. Kozlov, D. Darriba, T. Flouri, B. Morel, A. Stamatakis, RAxML-NG: A fast, scalable and
1059 user-friendly tool for maximum likelihood phylogenetic inference. *Bioinformatics* **35**,
1060 4453–4455 (2019).
- 1061 77. J. Felsenstein, Confidence limits on phylogenies: An approach using the bootstrap.
1062 *Evolution* **39**, 783–791 (1985).
- 1063 78. N. D. Patterson, M. Alipour, O. R. P. Bininda-Emonds, B. M. E. Moret, A. Stamatakis, How
1064 many bootstrap replicates are necessary? *Journal of Computational Biology* **17**, 337–354
1065 (2010).
- 1066
- 1067









A**B****C**